1   **The stele – a developmental perspective on the diversity and evolution of primary vascular**
2   **architecture**
3
4   Alexandru M.F. Tomescu
5
6   Department of Biological Sciences, Humboldt State University, Arcata, California 95521, USA
7   (+1) 707-826-3229   mihai@humboldt.edu
8
9   **Abstract**
10 The stele concept is one of the oldest enduring concepts in plant biology. This paper reviews the
11 concept and its foundations, and builds an argument for an updated view of steles and their evolution.
12 The history of studies of stelar organization has generated a widely ranging array of definitions of the
13 stele that determine the way we classify steles and construct scenarios about the evolution of stelar
14 architecture. Because at the level of the organism biological evolution proceeds by, and is reflected in,
15 changes in development, concepts of structure need to be grounded in development in order to be
16 relevant in an evolutionary perspective. For the stele, most of the traditional definitions that
17 incorporate development have viewed it as the totality of tissues that either originate from procambium
18 – currently the prevailing view – or are bordered by a boundary layer (e.g., endodermis). A definition of
19 the stele that would bring consensus between these perspectives recasts the stele as a structural entity
20 of dual nature. Here, I review briefly the history of the stele concept, basic terminology related to stelar
21 organization, and traditional classifications of the steles. I then revisit boundary layers from the
22 perspective of histogenesis as a dynamic mosaic of developmental domains. I use classic and recent
23 anatomical and molecular data to reaffirm and explore the importance of boundary layers for stelar
24 organization. Drawing on data from comparative anatomy, developmental regulation, and the fossil
25 record, I offer a model for a stele concept that integrates both the boundary layer and the procambial
26 perspective, consistent with a dual nature of the stele. The *dual stele model* posits that stelar
27 architecture is determined in the apical meristem by two major cell fate specification events: a first one
28 that specifies a provascular domain and its boundaries, and a second event that specifies a procambial
29 domain (which will mature into conducting tissues) from cell subpopulations of the provascular domain.
30 If the position and extent of the developmental domains defined by the two events are determined by
31 different concentrations of the same morphogen (most likely auxin), then the distribution of this
32 organizer factor in the shoot apical meristem, as modulated by changes in axis size and the effect of
33 lateral organs, can explain the different stelar configurations documented among tracheophytes. This
34 model provides a set of working hypotheses that incorporate assumptions and generate implications
35 that can be tested empirically. The model also offers criteria for an updated classification of steles that
36 is in line with current understanding of plant development. In this classification, steles fall into two
37 major categories determined by the configuration of boundary layers – boundary protosteles and
38 boundary siphonosteles, each with subtypes defined by the architecture of the vascular tissues.
39 Validation the dual stele model and, more generally, in-depth understanding of the regulation of stelar
40 architecture, will necessitate targeted efforts in two areas: (i) the regulation of procambium, vascular
41 tissue, and boundary layer specification in all extant vascular plants, considering that most of the
42 diversity in stelar architecture is hosted by seed-free plants, which are the least explored in terms of
43 developmental regulation; (ii) the configuration of vascular tissues and, especially, boundary layers, in as
44 many extinct species and lineages as possible.
45
46 **1. Theoretical premises**
47   The stele concept was introduced by van Tieghem & Douliot (1886 a, b). The history of the
48 concept and of the classification of stele types, as well as most of the attending terminology, were

49   reviewed in detail by Beck et al. (1982) and Schmid (1982). According to Schmid (1982), the practice of
50   characterizing the stele as comprising the primary vascular tissues of axial organs and some associated
51   tissues – pith and interfascicular regions – can be traced to Brebner (1902), Farmer & Hill (1902), and
52   Schoute (1903). Currently, like in the past, some authors use the term stele to refer exclusively to the
53   vascular system (Esau 1965; Beck et al. 1982). While many of these authors regard the stele as including
54   only primary vascular tissues (i.e., primary xylem and phloem, the 'primary stele' of Bower 1908), others
55   have expanded the concept to include also secondary vascular tissues (Cronk 2009). In paleobotany,
56   stele often refers only to the primary xylem, as phloem is infrequently preserved in plant fossils (Beck et
57   al. 1982).
58   Here, I give the stele a dual definition, as the totality of primary tissues of axial organs (stems,
59   roots or undifferentiated axes) that are (1) derived from procambium and (2) circumscribed by boundary
60   layers. I exclude secondary tissues from the stele because they are indirect, later-ontogenetic
61   derivatives of the procambium; because they do not develop in all vascular plants; and also because
62   their inclusion does not enrich the stele concept in any of its fundamental developmental or
63   evolutionary implications.
64   The organization of mature plant tissues is the product of development. The primary tissues of
65   axial organs are patterned in apical meristems. Specifically, the architecture of mature vascular tissues,
66   which are the principal components of the stele, is the result of patterning of the procambium in the
67   apical meristem. Thus, a key to stelar organization resides in the procambial architecture established
68   during apical development. Another important aspect of stelar organization is the boundary that
69   circumscribes the fundamental histogenetic domain from within which procambium will be specified
70   (referred to as the provascular domain below; see Section 6: Stele types and boundary layers). Such
71   boundary layers, also established during apical development, can provide another key to stelar
72   organization. However, though discussed by early workers (e.g., Tansley, 1896), the importance of
73   boundary layers has been subsequently downplayed, so that currently the prevailing views emphasize
74   only the procambial origin of the stele.
75   Within the framework provided by the view that procambial architecture is the main
76   determinant of stelar organization, the geometry of the procambium in the apical meristem region
77   provides the main criterion for defining stele types. This follows the ideas of Beck et al. (1982), who
78   advocated using the architecture of the procambium (or of the protoxylem) for comparing and
79   classifying stelar patterns. A classification of stele types based on procambial architecture typically
80   includes three main types of stele.
81
82   **2. Procambial architecture: three main types of stele among tracheophytes**
83   At the apices of axial organs, the procambium exhibits one of three main architectural
84   configurations that correspond to three main stele types. A **protostele** is a stele derived from a solid
85   central strand of procambium (Fig. 1a). The procambium is surrounded by ground meristem that
86   matures into the cortex. Vascular strands (leaf traces) may diverge from the stele to supply leaf bases.
87   A **siphonostele** develops from a hollow cylinder of procambium (Fig. 1b, 2). Aside from ground
88   meristem that differentiates into the cortex that surrounds the stele, siphonostelic axes also possess a
89   central cylinder of ground meristem that forms the mature pith. Another defining feature of the
90   siphonostele is the leaf gap, a discontinuity in the stele immediately above the point of divergence of
91   the trace(s) to a leaf (Fig. 2); the gap is a parenchymatous area and has limited longitudinal extent as it
92   "closes" distal to the leaf trace divergence (Beck et al. 1982). A **eustele** is a stele derived from a number
93   of discrete procambial strands (Fig. 1c). In cross sections, the strands taken together describe a more-
94   or-less circular outline that separates an outer cortex and a central pith, both derived from ground
95   meristem. The parenchymatous areas between adjacent vascular strands are termed interfascicular
96   areas (or pith rays, sometimes). The discrete strands of vascular tissue that comprise the stele (referred

97   to as cauline bundles) and the leaf traces that diverge from them are referred to as sympodia and can
98   form complex patterns. A segment of a cauline bundle between two successive leaf traces is also
99   referred to as a sympodial segment or reparatory strand (Namboodiri & Beck 1968). It is important to
100 note here that in eusteles the divergence of a leaf trace does not produce a leaf gap (see also Section
101 2.3: Eusteles).
102
103 **2.1. Protosteles**
104   Protosteles are divided, based on the cross-sectional geometry of the primary xylem (Fig. 3),
105 into haplosteles, actinosteles, and plectosteles. In haplosteles, the xylem has circular to oval shape in
106 cross section (Fig. 3a), in actinosteles it has a lobed (ribbed) shape (Fig. 3b), and in plectosteles it is
107 irregularly dissected into lobes and bands (Fig. 3c) that may anastomose along their trajectory through
108 the axis. The earliest tracheophytes of the Silurian and Devonian had axes with protostelic vasculature
109 (Stewart & Rothwell 1993). Among extant plants, protosteles characterize the stems of lycophytes,
110 psilotophytes, and some ferns (e.g., *Lygodium*). Even among siphonostelic ferns, the early growth stages
111 of some species have protosteles (e.g., *Gleichenia*). A protostele is also the vascular architecture that
112 characterizes the selaginellalean rhizophore and the roots of all tracheophytes, living and extinct.
113
114 **2.2. Siphonosteles**
115   Siphonosteles of different types characterize the stems of most ferns. Depending on the
116 longitudinal density of leaf gaps, siphonosteles are classified into solenosteles and dictyosteles.
117 Solenosteles exhibit no more than one leaf gap at any given level (i.e., in any cross section), whereas
118 dictyosteles can have two or more leaf gaps at the same level. In extreme cases, where multiple leaf
119 gaps occupy a higher proportion of the stele circumference than the sectors occupied by vascular tissue
120 [meristeles sensu Tansley (1907, 1908); see Beck et al. (1982)], such dictyosteles can look misleadingly
121 similar to a eustele, in individual cross sections; e.g., *Diplazium* or *Blechnum* (White & Weidlich 1995), or
122 the fossil *Dickwhitea* (Karafit et al. 2006).
123   Solenosteles and dictyosteles can be polycyclic, that is, consisting of two or more concentric
124 hollow cylinders of vascular tissue (e.g., Marattiaceae, Matoniaceae). In such cases, vascular bundles
125 forming leaf traces can diverge from one or several of the stele cycles (e.g., *Matonia*). Adjacent vascular
126 cylinders of a polycyclic siphonostele can be connected by connective bundles (e.g., *Saccoloma*, *Pteris*;
127 Troop & Mickel 1968). Furthermore, typical siphonosteles of different kinds, whether polycyclic or not,
128 can be variously combined with vascular segments that run along the central pith area (medullary
129 bundles; e.g., *Cyathea*, *Alsophila*, *Platycerium*) or, in some cases, the latter can be occupied by a central
130 vascular cylinder, like in a protostele (e.g., *Thyrsopteris*, *Matonia*). All these varieties have been
131 discussed, illustrated, and classified by many, including Bower (1923), Ogura (1972), and Schmid (1982).
132
133 **2.3. Eusteles**
134   Eusteles characterize the stems of all living seed plants. One topic of confusion in discussions of
135 eustelic organization has been the presence of leaf gaps. Some textbook treatments of stelar
136 architecture have perpetuated the idea that eusteles have leaf gaps, a leftover from the earlier view of
137 the eustele as a subtype of siphonostele (Esau 1977) and from classifications based on nodal
138 architecture. These views were also fueled by the inclusion of secondary tissues in the stele concept
139 (Esau 1965) and by observations of eusteles in which numerous cauline bundles and leaf traces give the
140 appearance of a continuous layer of vascular tissues (a condition termed pseudosiphonostely; Beck et al.
141 1982). However, careful studies of protoxylem architecture (e.g., Benzing 1967a, b) have demonstrated
142 the eustelic nature of pseudosiphonosteles, and the inclusion of secondary tissues does not enrich the
143 stele concept (for reasons discussed above – Section 1: Theoretical premises). Thus, my view is that
144 eusteles do not have leaf gaps.

145   Longitudinal sections through eustelic axes can produce vascular tissue configurations that look
146   misleadingly like leaf gaps (Fig. 4a, b) for two reasons. First, in the typical sequence of tissue
147   differentiation behind the shoot apical meristem, nodal tissues mature earlier than those of the
148   internodes. As a result of this, a procambial strand that is conspicuous in a node can appear to lose its
149   substance basipetally, along its trajectory through the internode, and to reappear in the next node
150   below, the same configuration that one would expect to see if a leaf gap was present. Second, in most
151   seed plants, leaf traces diverge from cauline bundles in a tangential direction (Fig. 4c, bottom three
152   planes of section) before traversing the cortex in a radial direction and upwards (Fig. 4c, top three
153   planes of section). This leads to tangential displacement of the cauline bundle above the divergence, as
154   a result of which the cauline bundle shows a hiatus immediately above (distal to) the node in
155   longitudinal sections (Fig. 4b), similar to that produced by a leaf gap in a siphonostele longitudinal
156   section.
157   Building on the basic sympodial architecture seen in Carboniferous seed ferns and even in
158   Devonian progymnosperms (e.g., Beck 1970, 1971, 1979), the various trajectories of seed plant
159   evolution and diversification have produced a tremendous diversity of eusteles. The sources of this
160   diversity are (1) the increase in the number of sympodia; (2) variations in the connectivity of sympodia,
161   which ranges from discrete unconnected sympodia, to random interconnections (by minor or accessory
162   bundles), to regular anastomoses between cauline bundles or between leaf traces and cauline bundles
163   (e.g., Beck et al. 1982); (3) leaf traces, although not technically part of the stele, can contribute
164   complexity to the stem vascular system, depending on whether they consist of single or multiple
165   bundles, whether these bundles diverge from single or multiple cauline bundles, and whether the traces
166   are short or long (i.e., traversing more than one internode between their divergence from the cauline
167   bundle and their entry into a leaf base). These compounded layers of complexity and diversity have
168   been encompassed in several classification systems (e.g., Schmid 1982). One such classification that
169   dominated the first half of the 20th century was based on nodal anatomy – the architecture of vascular
170   tissues at nodes. Skepticism about the philosophical and methodological bases of this classification,
171   along with the realization that nodal types are adaptive (thus, similar types may not be morphologically
172   equivalent), led to the conclusion that nodal anatomy, by itself, does not provide a conclusive
173   representation of stelar architecture in the absence of internodal features (Beck et al. 1982).
174   Given the diversity of eustelic architectures, it is important to remember that they all are
175   variations on the same basic sympodial organization. One such variation is seen in the atactostele of
176   some monocots, in which cauline bundles occurring in high numbers undulate in radial planes along
177   their trajectory through the stem. This, along with the emission of numerous, long leaf traces, produces
178   a highly complex organization wherein a multitude of vascular bundles are scattered throughout the
179   ground tissues of the stem, precluding a distinction between pith and cortex. The eustelic organization
180   of atactosteles has been demonstrated by Beck et al. (1982). Although this may be a slight
181   oversimplification, an atactostele can be visualized as a polycyclic eustele with multiple concentric cycles
182   of sympodia.
183
184   **3. A bit of history**
185   Concepts and classifications of steles initiated based on studies of extant plants in the 19th
186   century, gained added impetus in the second half of the 20th century by the contributions of
187   paleobotanists (e.g., Namboodiri & Beck 1968, Rothwell 1976; Beck et al. 1982), who brought fossil
188   lineages and their vascular architectures to the forefront of discussions of stelar morphology and
189   evolution. This synthesis opened the way to a broader, more inclusive and temporally-constrained
190   perspective on the diversity of stelar architecture and its evolution. Importantly, from their early
191   origins, discussions of stele classification have been firmly rooted in evolutionary views that fit within
192   the same broad paradigm as the modern evo-devo approaches.

193   Early on, Jeffrey (1899) recognized two main stele types, the protostele and the siphonostele, a
194   view shared by many morphologists in the early 20th century (Gwynne-Vaughn 1901; Brebner 1902;
195   Tansley 1907, 1908; Bower 1908). Focusing on the deep, early evolution of the vascular system, these
196   workers were not very concerned with the eustele that they regarded as a highly modified siphonostele
197   which, in turn, had evolved from a protostele. In contrast to this view, Boodle (1901), Scott (1902), and
198   others, regarded the eustele as having evolved from a protostele on a parallel trajectory to that of the
199   siphonostele, more consistent with the tripartite protostele-siphonostele-eustele classification.
200   Nevertheless, the scenario of eustele evolution from protosteles favored by these authors required
201   parenchymatization of central tissues associated with formation and expansion of leaf gaps, thus
202   implying a virtually siphonostelic intermediate stage. This view was only different from Jeffrey's ideas in
203   the mechanism proposed for the evolution of the intermediate stage – central parenchymatization, as
204   opposed to the "cortical invasion" process proposed by Jeffrey (see Beck et al. 1982). An origin of the
205   eustele from protosteles was also considered by Posthumus (1924) and, later, by Namboodiri & Beck
206   (1968), among others. The mechanism proposed by these authors involves ribbing of a protostele and
207   longitudinal dissection to form sympodia (see Section 7.2: Evolution of the pith – siphonosteles and
208   eusteles).

209
210   **4. Histogenesis as a dynamic mosaic of developmental domains**
211   Development in multicellular organisms leads to an organismal body comprised of populations
212   of terminally differentiated cells of different types. During this process, cell differentiation progresses
213   through successive cell fate decision steps. Considered in ontogenetic time, such stepwise cell fate
214   commitment sequences entail increasingly more distinct identity specification, coordinated within well-
215   circumscribed populations from within volumes of cells that can be regarded as equipotential fields in
216   terms of prior cell fate. These well-circumscribed cell populations represent domains defined by the
217   specific regulatory modules that determine their cell fate. In this context, a developing multicellular
218   body can be regarded as a mosaic of developmental domains. These domains define cell volumes in
219   which the same (set of) regulatory module(s) are expressed at a given moment in ontogenetic time. In
220   this spatially and temporally dynamic mosaic, developmental domains that succeed each other in
221   ontogenetic time can be (partially) overlapping or entirely disjunct.
222   In plants, the indeterminacy of meristematic growth requires continued circumscribing and
223   specification of developmental domains within the "flow" of new undifferentiated cells produced by the
224   meristem. Generation of a coherent plant body in this mode of growth requires maintenance of
225   longitudinal continuity, both anatomically and physiologically. Given these developmental constraints,
226   specification and maintenance of boundaries that define distinct developmental domains at any given
227   point in time is important throughout the successive levels of increasingly more advanced
228   differentiation, in increasingly smaller and more specific developmental domains of tissue and cell
229   identities.

230
231   **5. The importance of boundary layers**
232   If procambial architecture is a key determinant of stelar organization and provides a workable
233   criterion for defining stele types, these discussions cannot exclude consideration of the boundary layers
234   that separate the developmental domain from within which the procambium is specified, from the
235   adjacent ground tissues. Early on, this was a prevailing view (e.g., Tansley, 1896). However, subsequent
236   treatments concluded that boundary layers, such as the endodermis, had been given undue emphasis
237   and should not be used as criteria in discussions of stelar concepts, a view taken in the most recent
238   exhaustive analysis of stelar concepts by Beck et al. (1982).
239   My view is that boundary layers are important in discussions of stelar architecture. This view
240   rests on the crucial roles that boundaries and their regulation play throughout plant development – e.g.,

241   as demonstrated recently for leaf development (Caggiano et al. 2017). In support of this view,
242   accumulating evidence demonstrates that boundary layers, alongside other regulatory systems (auxin
243   and other hormones, tissue or cell identity specifiers, etc.), play an important role in determining the
244   extent and shaping the organization of the stele. For instance, in roots, miR165/166 produced in the
245   endodermis antagonize HD-ZIP III genes (C3HDZ hereafter) that determine procambial identity
246   (Carlsbecker at al. 2010; Miyashima et al. 2011), limiting their expression domain and, thus, determining
247   the volume occupied by procambium. Additionally, by inducing different C3HDZ dosage in different
248   regions of the stele, miR165/166 also specify protoxylem v. metaxylem fates (Hisanaga et al. 2014).
249   The layers that mark boundaries between the vascular tissues and ground tissues – the
250   endodermis in roots, the starch sheath in stems, and the bundle sheaths of leaf veins – are continuous
251   throughout the plant body (Fig. 5), despite having distinct physiological functions. Available evidence
252   suggests that they are specified by the same regulatory modules throughout the plant body (reviewed
253   by Tomescu 2008) and this shared developmental regulation indicates that they may be serially
254   homologous. Positionally, they are homologous with the endodermal layer that characterizes all the
255   organs of most seed-free plants. Furthermore, the regulation of C3HDZ genes by miR165/166 is shared
256   among all embryophytes (Floyd & Bowman 2004). This suggests that the antagonistic interaction
257   between miR165/166 and C3HDZ genes, which contributes to circumscription of the stele, is deeply
258   conserved and may have the same function in determining the extent and organization of the stele
259   across the entire tracheophyte clade. All this evidence strongly suggests that the boundary layer that
260   separates vascular tissues from ground tissues is a key determinant of stelar architecture. Thus,
261   contrary to earlier views, boundary layers should be thoroughly considered in definitions and
262   classifications of the steles.
263
264   **6. Stele types and boundary layers**
265   Primary vascular tissues are the principal components of the stele. They differentiate from
266   procambium, and so do other associated tissues typically included in the stele (e.g., the pericycle).
267   Together, these tissues are circumscribed by layers with specific identity, which separate them from
268   other tissues. These well-defined boundary layers, which extend throughout the plant body, indicate
269   the presence of two fundamentally distinct developmental domains: one referred here as the
270   *provascular domain*, because subpopulations of cells from within it generate vascular tissues, and an
271   *accessory domain*, consisting of ground tissues. In many axial plant organs, the provascular domain
272   coincides with the stele, thus, the boundary layer defines the extent of the stele.
273   Overlaying the boundary layer patterns onto the procambium architectural patterns supports
274   some of the stele types defined based on the latter, but also raises questions about some aspects of the
275   tripartite stele classification and some of the traditionally defined subtypes of the three major stele
276   types. Nevertheless, the dual perspective on stelar organization offered by taking into account both
277   procambial architecture and boundary layers provides an updated framework for evaluating hypotheses
278   on the evolution of vascular architecture and stele types.
279
280   **6.1. Protosteles**
281   In most protosteles, a well-defined endodermis separates the stele from the surrounding
282   ground tissues (Fig. 1a, 3, 7e). Exceptions, wherein an endodermal layer is less well defined, include
283   some species of the Lycopodiales and *Isoetes*. In the latter, the lack of axial elongation and the resulting
284   density of traces to appendages disrupt the stele-cortex limit to an extent that makes recognition of a
285   continuous boundary layer impossible. In most *Selaginella* species, the endodermis of stems is modified
286   to form a trabeculate layer that includes large air spaces. Additionally, in several species of *Selaginella*,
287   the stele is dissected into discrete plate-like meristeles, each surrounded by an endodermal layer.

288   A special case is that of protosteles that exhibit a central core of parenchymatous tissue, as seen
289 in certain monocot roots (e.g., *Zea*) or psilotophyte axes (*Tmesipteris*, *Psilotum*). This tissue can be
290 interpreted as a pith, suggesting that the stele is in fact a siphonostele. However, the distinction of such
291 forms from siphonosteles and a case against such an interpretation is supported by several lines of
292 evidence: (1) the presence of a well-defined endodermis around the vascular tissues, separating them
293 from the cortex, and the absence of an equivalent boundary layer circumscribing the central
294 parenchymatous core and separating it from the surrounding vascular tissues; (2) gradual longitudinal
295 histologic transitions along the stems of some plants (e.g., *Gleichenia*; Bower 1908) from a typical
296 protostele, in which the center is occupied by xylem, to a central area of various sizes occupied by
297 parenchyma; (3) a common developmental origin of the vascular tissues and the central
298 parenchymatous area in a central strand of procambium. Thus, this type of anatomy is best interpreted
299 as a medullated protostele.
300
301 **6.2. Siphonosteles**
302   A significant divide among siphonosteles, from a developmental, structural, and evolutionary
303 standpoint, is that between ectophloic and amphiphloic siphonosteles. In ectophloic siphonosteles,
304 primary phloem is found only in a layer external to the primary xylem, whereas in amphiphloic
305 siphonosteles there are layers of phloem both externally and internally to the xylem. In some cases, this
306 separation based on the relative position of phloem and xylem reflects a deeper divide in terms of the
307 radial patterning of developmental domains. Whereas in amphiphloic siphonosteles endodermal layers
308 separate the tissues of the stele from both the cortex (an endodermis external to the outer phloem
309 layer) and the pith (an endodermis internal to the inner phloem layer), in the ectophloic siphonostele of
310 the Osmundaceae there is only one endodermis – between the vascular tissues and the cortex. Thus, if
311 the endodermis marks the boundary between major developmental domains – that generate the stele
312 and ground tissues (i.e., the provascular and accessory domain, respectively) –, then an amphiphloic
313 siphonostele (Fig. 7g) is a true siphonostele, whereas the ectophloic siphonostele of the Osmundaceae is
314 a medullated protostele (Fig. 7f). This view is supported by two lines of evidence. One is structural –
315 there are no gaps in the phloem and endodermis corresponding to the gaps in the xylem, thus, the stele
316 as a whole has no leaf gaps, like protosteles and unlike siphonosteles. The other line of evidence is
317 paleobotanical and consists of a transformational time series of fossil osmundaceous genera that go
318 back to the Permian documenting the progressive replacement of the central metaxylem of a protostele
319 by parenchyma (e.g., Kidston & Gwynne-Vaughan 1914; Miller 1971; Stewart & Rothwell 1993).
320   Other ectophloic siphonosteles seem to be true siphonosteles derived by reduction of the inner
321 phloem layer. If that is the case, we expect to still see a boundary layer that separates the xylem from
322 the pith in these plants. However, the latest comparative studies of the anatomy of ferns with such
323 stelar configurations – primarily Vittariaceae (e.g., *Vittaria*, *Antrophyum*) – date back to almost a century
324 ago and, as pointed out by Ogura (1972), the accounts of different authors are not entirely consistent.
325 Whereas some authors report presence of well-defined inner phloem and an inner endodermis, others
326 report reduced or absent inner phloem and endodermis (e.g., Williams 1927). Critical reevaluation of
327 these species is needed to test for the presence of a boundary layer based both on anatomical evidence
328 and on specific molecular markers.
329
330 **6.3. Eusteles**
331   An endodermis marked by Casparian strips is rarely seen in stems with eustelic organization
332 (Esau 1977). Nevertheless, substantial evidence from anatomy, physiology, and development indicates
333 the presence of a boundary layer that separates two major domains in eustelic axes – a central domain
334 that includes vascular tissues (the stele) and an outer accessory domain of ground tissues (cortex) (Fig.
335 7j, l) – and that provides positional cues crucial for cell fate specification in the establishment of radial

336   patterning. In the young portions of many eustelic stems, the innermost cortex layer forms a starch
337   sheath, which shares regulatory mechanisms for identity specification with the root endodermis (see
338   Section 3: The importance of boundary layers). Furthermore, starch sheath cells give histochemical
339   reactions similar to those demonstrated in the endodermis, and these cells can be induced to develop
340   like a typical endodermis (Van Fleet 1950).
341   Esau (1977) hypothesized that a boundary surrounding the central region of eustelic stems is
342   specified by chemical interaction between materials derived from vascular tissues and those present in
343   the cortex. Developmentally, the segregation of a ring of residual meristem (as seen in cross sections)
344   close behind the shoot apical meristem, from within which procambial strands are specified that
345   connect the stele to leaf primordia (Esau 1977), also suggests the presence of a continuous boundary
346   that delimits a central developmental domain, which includes the vascular tissues, from surrounding
347   ground tissues. Despite being frequently inconspicuous anatomically, this boundary provides positional
348   cues for radial tissue patterning, namely the specification of distinct identities in the two developmental
349   domains that it separates. This is clearly demonstrated in seemingly homogeneous, parenchymatous
350   interfascicular areas, wherein surgical inversion of radial polarity (i.e. cortical domain at the center,
351   central domain outwards) results in inverted polarity of the interfascicular cambium, which produces
352   secondary phloem inwards and secondary xylem outwards (Siebers 1971).
353   Together, these observations suggest that although vascular tissues are organized in discrete
354   vascular bundles, in eustelic axes the basic radial patterning of tissues includes only two domains
355   separated by a boundary layer – a central domain, which includes tissues that gives rise to the stele, and
356   an accessory external (cortical) domain – much like in a protostele. This conclusion has implications for
357   discussions of stele evolution and classification.
358
359   **6.4. Transferability of boundary layer identity**
360   In discussing the developmental and structural significance of boundary layers, and their
361   importance for understanding stelar organization, it is important to note that the identity of boundary
362   layers is transferrable and their position labile, as suggested by multiple lines of evidence. Stems of
363   some ferns (e.g., *Gleichenia*; Bower 1908) transition in their epidogenetic growth phase from a
364   protostele to a *bona fide* siphonostele. This transition that is associated with an increase in stem
365   diameter involves the specification of a pith area and an inner endodermis. Thus, a simple change in
366   size can lead to a major change in stelar organization within the same axis, by generating a central
367   developmental domain and the corresponding boundary layer that separates it from a reorganized
368   domain with vascular competency. Additionally, in some ferns where the vascular tissues form a hollow
369   cylinder, different species of the same genus (e.g., *Vittaria*, *Antrophyum*; Williams 1927; see also Section
370   6.2: Siphonosteles above) may possess only an external endodermis or both external and internal
371   endodermal layers, or even an intermediate, discontinuous internal endodermis. In such cases the
372   lability of the inner endodermal layer blurs the distinction between siphonosteles *sensu stricto* and what
373   could be considered medullated protosteles.
374   A comparable situation may be present in some eusteles, as Van Fleet (1961) reports cases
375   where an inner endodermis (also termed a medullary sheath) exists between the pith and the cauline
376   vascular bundles (e.g., *Clintonia*, *Maianthemum*) or can be induced experimentally (*Vicia*). Finally,
377   different species of the genus *Equisetum* (whose stelar architecture is discussed below; Section 8.2.4:
378   Additional complexity and unknowns) possess one of three possible endodermal configurations –
379   including one with an external endodermis and one with both external and internal endodermal layers.
380   Furthermore, these configurations may change within the same plant at the transition from the
381   underground rhizome to aerial shoots (reviewed by Tomescu 2008). Consistent with all these
382   observations that indicate positional lability and transferability of boundary layer identity, Drapek et al.
383   (2018) demonstrated that it is possible to induce formation of ectopic Casparian strips (interpreted as

384 reflecting endodermal identity) in subepidermal layers of *Arabidopsis* roots, and that the transcription
385 factor SHR and the ligand CIF2 are sufficient for this.
386
387 **7. Evolutionary considerations**
388
389 **7.1. The plesiomorphic protostele**
390   It is clear that the plesiomorphic stelar architecture is a protostele. The oldest known
391 tracheophytes have protosteles (Kidston & Lang 1917, 1920a, b; Edwards 1970, 1981; Banks et al. 1975;
392 Gensel 1976; Edwards et al. 1992; Strullu-Derrien et al. 2014; Matsunaga & Tomescu 2017). The sharp
393 transition that is obvious in these fossil plants between tissues with very different identities – those of
394 the stele and those of the surrounding cortex – indicates the presence of well-defined boundary
395 conditions, thus, it is likely that a mechanism for boundary layer specification existed in the early
396 protostelic tracheophytes. In fact, the protostele-type radial patterning of tissues pre-dates the
397 tracheophytes, as it is seen in plants that lack tracheids and sieve cells – protracheophytes (Boyce 2008;
398 Cascales-Miñana et al. 2019) and even bryophytes, both in the gametophyte and sporophyte phases
399 (Hébant 1977). In all these plants, the conducting tissues form a central cylinder, irrespective of the
400 identity and degree of specialization of these cells, thus, a protostele *sensu lato* is the plesiomorphic
401 condition of all axial plant organs. Indirect evidence for this also comes from studies of cell fate
402 determination in the pith of the *Arabidopsis* eustele (Sanchez et al. 2012). Here, the parenchymatous
403 identity of cells is maintained by the WRKY12 transcription factor, in the absence of which the cells
404 develop secondary walls (Wang et al. 2010), like the tracheary elements of the xylem. These data
405 suggest that the default identity of central tissues is similar to that of xylem, supporting the
406 plesiomorphic nature of the protostele. They also suggest a pathway for the evolution of the pith, by
407 suppression of vascular tissue identity at the center of the stele.
408
409 **7.2. Evolution of the pith – siphonosteles and eusteles**
410   Both siphonosteles and eusteles are characterized by the presence of a pith, thus, the evolution
411 of the pith is central to understanding the evolution of stelar architecture. Specifically, this entails
412 addressing when and by what mechanisms pith evolved. The fossil record provides clues relevant to
413 both of these aspects of pith evolution. In terms of timing, axes with a central core of parenchymatous
414 ground tissue are known in both lycophytes (i.e., lepidodendrid isoetaleans) and euphyllophytes
415 (archaeopteridalean progymnosperms, archaeocalamitacean sphenopsids, cladoxylopsids) by the end of
416 the Devonian. By Mississippian time, the seed plants include members that possess a central core of
417 parenchymatous tissue in their stems, and in the Pennsylvanian this feature is also present in several
418 fern groups (e.g., Marattiales, Filicales) (Stewart & Rothwell 1993). In terms of mechanism, a central
419 core of ground tissue is thought to have evolved either by parenchymatization of the central region of
420 the axis (also known as medullation) or by fragmentation of the central vascular tissues (also referred to
421 as dissection), in both cases starting from a protostele. These two mechanisms have been discussed in
422 relation to different lineages.
423   In ferns and lycophytes, evolution of the pith is thought to be the result of medullation. In
424 support of this view, the fossil record of osmundaceous ferns provides a compelling series of species
425 that illustrate progressive parenchymatization of the central region of rhizomes occupied by xylem
426 (Kidston & Gwynne-Vaughan 1914; Miller 1971; Rothwell 1992; Stewart & Rothwell 1993). Among living
427 ferns, the stem of a single plant may exhibit a size-dependent transition from a protostele with xylem at
428 the center, produced in thinner juvenile stages, to a siphonostele wherein the center is occupied by pith,
429 as the rhizome reaches its mature thickness (e.g., *Gleichenia*; Bower 1908). A similar size-dependent
430 transition from a *bona fide* protostele to a medullated protostele along the stems of single plants has
431 been documented in extinct lepidodendrid lycophytes by Eggert (1961). Progressive medullation (of an

432   actinostele) has also been proposed as the driver in the evolution of the pith in sphenopsids (reviewed
433   by Stewart & Rothwell 1993) (Fig. 7h, i), whereas among cladoxylopsids (see also Section 8.3.3: Radial
434   concentration and eusteles) the pith is thought to have evolved by a combination of fragmentation of an
435   actinostele (also referred to as dissection), as a first step, followed by medullation (Stewart & Rothwell
436   1993) (Fig. 7h, k, l). For both these lineages, evolutionary scenarios are based on transformational series
437   illustrated by fossil species and an increase in the size of axes may have been one of the drivers of the
438   evolution of the pith.
439   In the case of the seed plant eustele, the most widely accepted evolutionary scenario posits that
440   longitudinal dissection (fragmentation) of an actinostele produced a system of discrete cauline bundles
441   separated at the center by ground tissue, whose breadth expanded subsequently by progressive
442   medullation (Namboodiri & Beck 1968) (Fig. 7h, k, l). Seed plants are thought to have arisen from
443   progymnosperm precursors (Stewart & Rothwell 1993). However, progymnosperms fall within a few
444   lineages (Beck 1976) – most prominent of which are the aneurophytes and the archaeopterids – and the
445   relationships among these lineages, as well as between them and seed plants, are not fully understood
446   (Toledo et al. 2018).
447   The archaeopterids are considered eustelic (Rothwell & Erwin 1987), like the derived (and like all
448   extant) seed plants. However, thin archaeopterid stems possess medullated protosteles (actinosteles)
449   whose parenchymatous core widens out in larger stems, separating discrete xylem strands (Carluccio et
450   al. 1966; Scheckler 1978; Beck 1979). Thus, if archaeopterids are the sister group of seed plants, then
451   eusteles would have originated from protosteles directly by medullation not preceded by longitudinal
452   dissection (Fig. 7h, l, j). However, the oldest seed plants have protosteles (actinosteles; Serbet &
453   Rothwell 1992), like the aneurophyte progymnosperms. If seed plants are monophyletic, then their
454   stelar organization indicates a sister group relationship with the aneurophytes. In this case, the
455   sequence of protostele dissection and subsequent medullation (Fig. 7h, k, l) proposed by Namboodiri &
456   Beck (1968) and Beck (1970), and refined by Rothwell & Erwin (1987) and Rothwell (1992) with respect
457   to protoxylem architecture, best explains the origin of the eustele and its pith.
458   In all the cases discussed above, the development of a central parenchymatous area of the stele
459   is associated with an increase in axis diameter. This, as well as the evolution of specialized lateral
460   appendages (leaves), are thought to have imposed physiological constraints – underpinned by efficiency
461   of water and photosynthate transfer and by economy in the production of energy-demanding
462   specialized conducting tissues – that drove evolution of siphonosteles and eusteles (reviewed by
463   Decombeix et al. 2019). Below, I propose a model informed by current understanding of developmental
464   regulation and sensitive to axis size variation, to provide a unifying explanation for the nature of the
465   stele and its evolution that is consistent with both the procambial and the boundary layer views of the
466   stele discussed above.
467
468   **8. A unifying perspective on stelar architecture: the *dual stele model***
469   The dual stele model (Fig. 6) posits two cell fate specification mechanisms that are deployed
470   sequentially and delimit increasingly more narrowly circumscribed and more specialized developmental
471   domains. The first mechanism specifies a *provascular domain* (not to be confused with provascular
472   tissue, i.e., procambium – e.g. Scarpella et al. 2000), wherein cells maintain the competency to
473   differentiate into procambial tissue, and establishes a boundary layer that separates this domain from
474   the neighboring accessory domain. The second mechanism specifies *procambial identity* in cells within
475   the provascular domain that will differentiate into xylem and phloem. If the two developmental
476   domain-specifying mechanisms interact and are coordinated, at a higher level of regulation, by an
477   organizer factor acting in a dosage-dependent manner (see Section 8.2: Connections and coordination),
478   together, these conditions could explain the variety of stelar architectures present among
479   tracheophytes.

480

8.1. Potential developmental regulators

Current understanding of the regulation of radial tissue patterning and vascular tissue development points to potential molecular actors involved in the regulatory mechanisms of the dual stele model. The GRAS family transcription factor SHR could be the master regulator driving the first cell fate specification mechanism that leads to establishment of the provascular domain. SHR has been demonstrated to play an important role in cell division and specification within the stele (Levesque et al. 2006). SHR is produced in tissues that become part of the stele and moves outside of these tissues, activating another member of its gene family (*SCR*) at their periphery. Together, SHR and SCR establish the boundary layer (Di Laurenzio et al. 1996; Helariutta et al. 2000; Cui et al. 2007). The second mechanism, responsible for procambial identity specification, could be based on HD-ZIP III family genes (C3HDZ), which are emerging as the transcription factors at the center of the regulatory network required for initiating and maintaining vascular tissues (Ramachandran et al. 2017).

In the boundary layer, SHR and SCR activate *MIR165/166*. In turn, miRNA165/166 move into the provascular domain where they degrade C3HDZ mRNAs, thus circumscribing the expression domain of these genes (Carlsbecker et al. 2010) and, consequently, the procambial developmental domain that will generate the conducting tissues. As a counterbalance to the C3HDZ-miR165/166 interaction, miR165/166 are negatively regulated by *PNH* (an AGO family gene), which has an expression domain broadly overlapping with C3HDZs and protects them from silencing by miR165/166 (Ramachandran et al. 2017).

Evidence from multiple studies touching on different aspects of these regulatory roles and interactions (e.g., Fukaki et al. 1998; Helariutta et al. 2000; Scarpella et al. 2000; Wysocka-Diller et al. 2000; Floyd & Bowman 2004, 2007; Juarez et al. 2004; Levesque et al. 2006; Cui et al. 2007; Carlsbecker et al. 2010; Muraro et al. 2014, and many others), reviewed in several papers (e.g., Tomescu 2008; Sanchez et al. 2012; Ramachandran et al. 2017; Campbell & Turner 2017), shows that they are deployed across all sporophyte organs and wide spread among different plant lineages. Although the picture they paint is still incomplete, when considered collectively these studies strongly suggest that the interactions described above are conserved across vascular plants and may, thus, provide a plausible regulatory framework within which to explore the evolution of stelar architecture.

8.2. Interactions and coordination

If the regulatory interactions outlined above are sufficient to determine the extent and geometry of the stele, then they include two aspects that are particularly important for the definition and classification of stele types. First, the two cell fate specification mechanisms that determine the provascular and procambial domains are connected through the intermediary of boundary layers, wherein the provascular domain specifier (SHR) activates a factor (miR165/166) that inhibits the activity of the procambial domain specifier (C3HDZ) (Fig. 6), thus constraining the physical extent of this domain. Second, another unifying aspect is the presence of a putative higher level organizer – auxin. Ample evidence indicates that C3HDZ gene expression is induced by auxin through the intermediary of auxin response factors, such as MP (Baima et al. 1995; Mattsson et al. 2003; Donner & Scarpella 2009), and, in turn, C3HDZs promote developmental changes that support auxin canalization (e.g., Ilegems et al. 2010; Ramachandran et al. 2017). It is unclear what factors act upstream of SHR, but given that (1) the expression domain of SHR consistently includes the procambial domain and (2) polar auxin transport has a key role in shaping this domain, it is likely that SHR has significant interactions with auxin, as suggested by some studies (Levesque et al. 2006; de Luis Balaguer et al. 2017). Thus, it is possible that auxin acts the organizer coordinating the two regulatory mechanisms (Fig. 6). Consistent with this, radial patterning of the *Arabidopsis* root requires integration of the SHR-miR165/166-C3HDZ interactions network with auxin signaling (Muraro et al. 2014). These connections, some of which are demonstrated

528   while others are more putative, indicate that only integration of aspects of both boundary layers and
529   procambial architecture into stelar concepts can lead to deeper understanding of the regulation and
530   evolution of stelar architecture, in the model proposed here.
531
532   **8.3. Applying the dual stele model to stele types and reconciling existing data and hypotheses**
533
534   **8.3.1. Protosteles and auxin redistribution**
535   In a protostele, the provascular and procambial domains overlap in the central area of the axis
536   (Fig. 7e), with the exception of a layer that is part of the provascular domain but falls outside the
537   procambial domain and forms the pericycle – bordered by the boundary layer (endodermis). This is
538   consistent with the SHR-miR165/166-C3HDZ interactions demonstrated in roots. Furthermore, the
539   same interactions have also been reported in leaf veins (Wysocka-Diller et al. 2000; Gardiner et al.
540   2011), which represent cylindrical vascular bundles surrounded by a boundary layer (the bundle sheath)
541   analogous to a protostele. The idea that the procambial domain specifiers – C3HDZs – mediate "central
542   cell fate" (Sanchez et al. 2012), including vascular tissue identity, in the sporophytic axes of early land
543   plants is consistent with the protostelic organization of the earliest tracheophytes (see Section 7.1: The
544   plesiomorphic protostele). Because leaves evolved independently in euphyllophytes and lycophytes
545   (Tomescu 2009), in which C3HDZs are key to development of the protostelic vascular system (Floyd &
546   Bowman 2006), the role of C3HDZs in regulating vascular programs in the stem predates any roles in
547   leaves (Sanchez et al. 2012).
548   Development of steles with a parenchymatous central area – medullated protosteles,
549   siphonosteles, and eusteles – could be explained by a common organizer factor that specifies the two
550   developmental domains (provascular and pocambial) in a dosage-dependent manner, activating the
551   provascular domain specifier at lower concentrations and the procambial domain specifier at higher
552   concentrations (Fig. 6). Under these constraints, a limited supply of organizer factor could explain these
553   different stele types as a function of axis size and the influence of lateral appendages on the distribution
554   of organizer concentrations. Auxin is a strong contender for the organizer factor, as discussed above,
555   and auxin homeostasis at the shoot apical meristem may well function based on a limited auxin supply
556   for which multiple sinks compete (Reinhardt 2005).
557   An increase in the demand of auxin per cross-sectional area of an axis would result in
558   redistribution of auxin concentrations that would, in turn, lead to the reorganization of the
559   developmental domains that determine the patterning of stele tissues (Fig. 7b, c, d). Assuming that the
560   apical meristem area is the main source of auxin, such a disturbance of auxin concentrations could be
561   induced by an increase in axis size unmatched by a corresponding increase in apical meristem size.
562   Irrespective of the underlying cause, redistribution of auxin concentration typical of a protostele in a
563   larger axis under the constraint of limited supply could follow one of two pathways. *Peripheral*
564   *concentration* would lead to depletion of auxin in the central region of the axis, to maintain high enough
565   concentrations for procambial specification around the periphery of this area (Fig. 7b, c). *Radial*
566   *concentration* would lead to depletion of auxin along radial sectors, leaving a ribbed central area with
567   auxin concentrations high enough for provascular and procambial specification (Fig. 7b, d).
568   The factor influencing which of the two pathways is deployed by a plant lineage may be the
569   effect of lateral appendages on the distribution of auxin in the apical meristem, in terms of their
570   strengths as sinks or sources. This is consistent with evidence for independent evolution of leaves in
571   ferns and seed plants (Tomescu 2009), whose stelar architectures illustrate peripheral and radial
572   concentration, respectively (see Sections 8.2.2 and 8.2.3 below). In contrast to these euphyllophyte
573   lineages, leaves seem to have little influence on auxin distribution and the structure of the protostele of
574   lycophytes (Floyd & Bowman 2006, 2010; Gola et al. 2007), consistent with their independent evolution
575   in this lineage. These observations point to the importance of the relationships between lateral

576   appendages, with their influence on concentrations of auxin and other putative morphogens in the
577   shoot apical meristem, and stelar architecture. Although not explored in further detail in this chapter,
578   these interactions require further attention.
579
580   **8.3.2. Peripheral concentration and siphonosteles**
581   Peripheral concentration of auxin (Fig. 7b, c) would lead to stelar configurations of the
582   medullated protostele and siphonostele type (Fig. 7f, g). If the central depletion does not take auxin
583   concentration below levels required for activation of the provascular domain specifier, the axis will still
584   possess a central provascular domain bordered by an endodermal layer (Fig. 7f). However, the lower
585   central concentration of auxin will limit specification of the procambial domain (which requires higher
586   auxin concentrations) to the periphery of the provascular domain, as seen in the medullated protosteles
587   of osmundaceous ferns and lepidodendrid lycophytes (in which an endodermis has yet to be
588   demonstrated). The size-dependent medullation in lepidodendrids and the transformational series
589   leading to medullation in fossil Osmundaceae both illustrate this type of stelar transition and
590   demonstrate its developmental feasibility within a plant, as well as in evolutionary time. Severe auxin
591   depletion at the axis center would limit specification of provascular identity to a hollow cylinder of
592   tissue. SHR produced in this reduced provascular domain would then move into adjacent tissues both
593   outwards and inwards, establishing two boundary layers – the outer and inner endodermis
594   characteristic of siphonosteles – and constraining the extent of the procambial domain also between
595   these two layers (Fig. 7g). The size-related transition from protosteles to siphonosteles along *Gleichenia*
596   rhizomes (Bower 1908) could reflect severe auxin depletion due to peripheral concentration. Cases such
597   as the Vittariaceae (see Section 6.4: Transferability of boundary layer identity) suggest that in some
598   cases development (or evolution) of a siphonostele may go through an intermediate medullated
599   protostele stage (Fig. 7f, g). On the other hand, in siphonostelic ferns experimental suppression of leaf
600   primordia, disturbing the patterns of distribution of auxin produced in the shoot apical meristem
601   (Wardlaw 1946; Soe 1959; Ma & Steeves 1992), leads to loss of the characteristic leaf gaps and even to
602   protostelic organization, in severe cases (Ma & Steeves 1992, 1995), consistent with a key role of leaves
603   in determining the distribution of auxin concentrations and, through them, stelar organization.
604
605   **8.3.3. Radial concentration and eusteles**
606   Radial concentration of auxin (Fig. 7b, d) would lead to actinostele-type configurations, wherein
607   the vascular tissues form a central column with longitudinal ridges (ribs) and grooves, wrapped in a
608   boundary layer (Fig. 7h). Records of Early Devonian plants with a ribbed column of central xylem
609   (Gensel 1984; Remy & Hass 1986; Bickner & Tomescu 2019) place the origin of actinosteles as far back in
610   time as 400 million years. Higher in the stratigraphic column, actinosteles are present in multiple
611   lineages: cladoxylopsids (iridopterids and some pseudosporochnaleans), stenokolealeans,
612   progymnosperms (aneurophytes and archaeopterids), and early seed plants.
613   Archaeopterids present a special case indicating that radial concentration and peripheral
614   concentration are not mutually exclusive. *Actinoxylon*, a Middle Devonian putative archaeopterid
615   (Matten 1968) possesses an actinostele whose central area is occupied by parenchyma with a few
616   scattered tracheids. Even more dramatic is the progressive medullation of the actinostele along
617   archaeopterid stems, as they increase in size distally (Scheckler 1978). These examples suggest that the
618   archaeopterid lineage descended from ancestors in which stelar development followed the radial
619   concentration pathway (Fig. 7d, h). Deployment of the peripheral concentration pathway (Fig. 7h, i, j), in
620   the same way as in medullated protosteles, as a morphogenetic program overprinting the
621   developmental domains generated by radial patterning, subsequently led to a eustelic configuration in
622   archaeopterids.

623   The seed plant eustele, the dissected stele of some cladoxylopsids (referred to as a eustele by
624   some; Decombeix et al. 2019), and the stele with discrete vascular bundles present in many
625   sphenopsids, may have arisen along a path similar to that seen in archaeopterids – combining radial
626   concentration and peripheral concentration –, as implied by transformational series and evolutionary
627   scenarios based on fossils (Stewart & Rothwell 1993). However, in contrast to the archaeopterid
628   pathway, the scenarios proposed for seed plants (Namboodiri & Beck 1968; Beck 1970) and
629   cladoxylopsids, involve initial fragmentation (dissection) of the actinostele – corresponding to more
630   severe radial concentration – followed by development of a central parenchymatous area due to
631   subsequent peripheral concentration (Fig. 7h, k, l). Furthermore, the medullary sheath reported by Van
632   Fleet (1961) in some angiosperm stems to the inside of the ring of vascular bundles of the eustele, could
633   represent the equivalent of the inner endodermis of siphonosteles, if its boundary layer identity is
634   confirmed. Like in siphonosteles, medullary sheaths would indicate severe auxin depletion at the axis
635   center, as a result of peripheral concentration, that limits specification of provascular identity to a
636   hollow cylinder.
637   A series of studies have addressed the important role of lateral appendages and their mark on
638   apical meristem auxin concentrations, in shaping the actinostele and the evolutionary trajectory leading
639   to the eustele. Wight (1987) proposed that ribbing of a terete protostele to produce an actinostele was
640   driven by changes in development induced by the effect of lateral appendages on the distribution of
641   auxin concentrations at the axis apex. Rothwell (1992) expanded this evo-devo view to explain the
642   evolution of the seed plant eustele from an actinostele in parallel with the evolution of leaves, and
643   associated changes in protoxylem architecture encompassing the transition from the typical "radiate
644   protoxylem" organization (Beck & Stein 1993) to the discrete sympodia seen in eustelic seed plants. At
645   the same time, Stein (1993) used modeling to identify a small number of parameters controlling auxin
646   dynamics at the apical meristem and responsiveness of target tissue to auxin concentrations, whose
647   variations produce the types of stelar organization predicted in the scenarios of Beck (1970), Wight
648   (1987), and Rothwell (1992).
649   Contrary to the eustele evolution scenario proposed for early seed plants, which suggests radial
650   concentration with subordinated peripheral concentration, the development of the angiosperm eustele
651   indicates a different pathway. In *Linum*, the developmental sequence documented by Esau (1977) in the
652   shoot apex shows a ring-shaped residual meristem from within which procambiun stands are specified
653   subsequently. If the residual meristem corresponds to the provascular domain or its periphery, this
654   developmental sequence suggests that radial concentration – specifying individual procambium bundles
655   – follows (is subordinated to) peripheral concentration that specifies the residual meristem. This
656   reversed sequence (as compared to that proposed for early seed plants) could reflect the highly derived
657   condition that the angiosperm eustele represents among seed plant steles, which may be the result of
658   heterochronic change in the deployment of radial and peripheral auxin concentration pathways. As the
659   procambium strands that differentiate within the residual meristem are associated with leaf primordia
660   and differentiate into leaf traces, the radial concentration path seems to be controlled by the lateral
661   appendages in the development of the angiosperm eustele.
662
663   **8.3.4. Additional complexity and unknowns**
664   The stelar configurations of some extant and fossil plants continue to be difficult to fit into any
665   stele classification. The steles of the extinct cladoxylopsids, especially non-iridopterid representatives,
666   can be very complex (Bertrand 1935; Leclercq & Banks 1962; Soria & Meyer-Berthaud 2003; Xu et al.
667   2017) and have been likened to plectosteles and eusteles. The scenarios proposed to date to explain
668   their evolution are too simplistic to encompass the broad diversity of structures documented in the
669   group, which is ripe for reassessment in an evolutionary developmental framework.

670   Among living plants, *Equisetum* has puzzled students of plant structure in many respects and its
671   stelar architecture is no exception. In the nodes of its jointed stems, the vascular tissues seem to form a
672   siphonostele, whereas the internodes possess discrete vascular bundles, like those of a eustele (Unger
673   1856; Barratt 1920; Bierhorst 1971). Additionally, different species possess one of three endodermal
674   configurations, which can also differ between aerial shoots and rhizomes in the same plant (Ogura 1972;
675   Tomescu 2008). The key to understanding the stelar architecture of *Equisetum* may reside in the
676   particular mode of growth of the shoots of these plants, which arise from the concerted activity of two
677   types of meristems: an apical meristem that lays down a stack of phytomers, and intercalary meristems
678   that fuel the elongation of the internode in each phytomer (Tomescu et al. 2017).
679   Within this developmental framework, the stele with double endodermis (as an example) of an
680   *Equisetum* stem could be explained, by the following sequence (Fig. 8): initial specification of a central
681   provascular domain within young phytomers in early stages of radial patterning and subsequent
682   peripheral concentration leading to a hollow cylinder of provascular domain; specification of inner and
683   outer endodermal layers, at the stage of phytomer differentiation into a lower internode tier and an
684   upper nodal tier, in the latter; procambial domain specification in the nodal tier between the two
685   endodermal layers, as leaf primordia emerge, while the internode tier remains meristematic, forming an
686   intercalary meristem; in growing internodes, acroscopic production of new tissue by the intercalary
687   meristem at high rates and fast internode elongation maintain low levels of auxin in the provascular
688   domain (hollow cylinder), precluding specification of procambial domain between the two endodermal
689   layers; procambial strands differentiate within the provascular domain of the internode along vertical
690   lines corresponding to, and under the influence of, leaf primordia. This hypothetical sequence can be
691   tested once the molecular specifiers for the provascular and procambial domains are identified in
692   *Equisetum* and their expression patterns are documented.
693
694   **9. An updated classification of steles outlined**
695   Applied to stelar classification, the notion that the stele comprises all tissues delimited by the
696   boundary layer(s) results in a dichotomy that recognizes two basic configurations in which the
697   provascular domain either forms a central cylinder or a hollow cylinder. At first glance, this bipartite
698   scheme, which harkens back to the early views of Jeffrey (1899), provides an alternative to the tripartite
699   scheme based on procambial architecture. However, this boundary layer-based view is grounded in
700   development and cell fate specification just as much as the procambial perspective. Neverthless, in the
701   dual stele concept discussed in the preceding sections the former operates at a higher level of generality
702   than the latter. Here, I propose an updated classification that takes into account these considerations,
703   based on the dual stele concept.
704   To avoid introducing unnecessary additional terms, I refer to the two major types of steles
705   corresponding to the two basic configurations of the provascular domain – and its boundary layer(s) – as
706   *boundary protosteles* (central cylinder of provascular tissue with only one boundary layer at the
707   periphery) and *boundary siphonosteles* (hollow cylinder of provascular tissue delimited by inner and
708   outer boundary layers) (Fig. 7).
709   Boundary siphonosteles correspond, for the most part, to *bona fide* siphonosteles seen in many
710   living ferns, i.e., amphiphloic siphonosteles wherein the procambial domain overlaps with the
711   provascular domain, except for the inner and outer pericycle layers (Fig. 7g). Stelar architecture in the
712   *Equisetum* example discussed above (Fig. 8; Section 8.3.4: Additional complexity and unknowns) also
713   corresponds to a boundary siphonostele. In this case, given the discrete vascular bundles that form the
714   vascular supply of internodes, their vascular organization would qualify as a *eustelic* boundary
715   siphonostele.
716   Boundary protosteles can fall within a number of subtypes, depending on the organization of
717   the procambium within the provascular domain (Fig. 7). *Haplostelic* boundary protosteles (Fig. 7e)

718   correspond to the typical protostele with a terete procambial strand, as in thin or young *Gleichenia*
719   stems, or the axes of fossil zosterophylls (e.g., *Zosterophyllum*) and trimerophytes (e.g., *Psilophyton*).
720   The steles of all roots are also haplostelic boundary protosteles. Their traditional designation as
721   actinosteles is a misnomer, as only their xylem, and not the procamium as a whole, is lobed (ribbed). A
722   more correct designation for root steles is as haplostelic boundary protosteles with lobed xylem. In the
723   same line of reasoning, the steles of *Lycopodium* or *Selaginella* stems, traditionally referred to as
724   actinosteles and plectosteles, are also haplostelic boundary protosteles with lobed or dissected xylem.
725   True *actinostelic* boundary protosteles (Fig. 7h) with a ribbed column of procambium are seen in
726   *Psilotum* and *Tmesipteris*, as well as in some extinct progymnoperms, stenokolealeans, and
727   cladoxylopsids. Other cladoxylopsids possess putative *plectostelic* boundary protosteles (i.e. dissected
728   column of procambium), although a single boundary layer surrounding all the vascular segments of an
729   axis would need to be identified unequivocally in these extinct plants for this assignment to be
730   validated.
731   In *siphonostelic* boundary protosteles (Fig. 7f), the procambium forms a hollow cylinder. This
732   assignment applies to the stelar organization of the traditional medullated protosteles of monocot
733   roots, and to the ectophloic "siphonostele" of the Osmundaceae and some other ferns (e.g., Vittariaceae
734   *pro parte*). If the large medullated axes of lepidodendraleans do not possess an internal boundary layer
735   separating the pith from the vascular tissues, then their organization also corresponds to siphonostelic
736   boundary protosteles.
737   Finally, because they are bordered only by an external boundary layer, seed plant eusteles also
738   qualify as boundary protosteles, designated here as *eustelic* boundary protosteles, in reference to the
739   discrete strands of protoxylem that differentiate within, and close to the periphery of, the central
740   provascular domain (Fig. 7j, l).
741   To be fully supported and, thus, become fully applicable, this classification based on
742   developmental features requires that some significant knowledge gaps are filled. On one hand, neither
743   procambial architecture nor boundary layers are easily documented or even preserved in the fossil
744   record, therefore the classification is not readily applicable to many fossils. Apical meristems
745   demonstrating procambial architecture are rarely preserved in the fossil record and, except for
746   endodermal layers with conspicuous thickenings, boundary layers are not easily identified in fossils.
747   Nevertheless, instances of excellent preservation of apical meristems (e.g., Melchior & Hall 1961;
748   Delevoryas 1964; Good & Taylor 1972; Dennis 1974; Edwards 1994; Slater et al. 2015; Hetherington et
749   al. 2016; Hetherington & Dolan 2018) indicate that continued exploration of the fossil record will reveal
750   more about procambial architecture in extinct plants. On the other hand, boundary layer identity seems
751   to be positionally labile (see Section 6.4: Transferability of boundary layer identity), and understanding
752   boundary layer specification across all tracheophyte lineages is still a remote target. Thus, the
753   classification I propose here is, for now, an outline. Nevertheless, a dual outlook on the stele that
754   combines the procambial view and the boundary layer perspective is developmentally grounded and can
755   inspire interesting perspectives on the evolution of stelar architecture that are worth pursuing. This
756   classification, alongside the dual stele model that it is derived from, forms an extended working
757   hypothesis toward this goal.
758
759   **10. Outstanding questions and future research**
760   Because of the paramount importance of conducting tissues in vascular plants, the stele is one
761   of the oldest enduring concepts in plant biology. Although the concept has generated much discussion
762   throughout its history and there is general agreement that the stele includes vascular tissues, current
763   definitions of it vary in specificity and inclusiveness. Among these, those that are grounded in
764   development – the only ones that are relevant in an evolutionary perspective –, emphasize either
765   boundary layers or, more prevalently, the procambium.

766   To reconcile these different views, I propose the dual stele model, a stele concept that
767   incorporates both boundary layers and procambium as originators and key components of the stele.
768   This model posits that the stele is determined by specification of provascular and procambial
769   developmental domains (the latter nested within, and regulated through inhibitors produced by, the
770   former) by lower and higher concentrations, respectively, of a coordinating organizer factor. The
771   proposed regulatory framework for the dual stele model is based on current understanding of the
772   molecular-genetic regulation of boundary layer and procambium identity in a few angiosperm species.
773   Thus, the model is a set of working hypotheses. Testing of these hypotheses and refining of the model,
774   if confirmed, will require development of new data in two major directions of investigation.
775   One of these directions addresses the regulators of procambial, vascular, and boundary layer
776   identity. The full system of interactions between these regulators requires some refining even in
777   angiosperms, wherein it is well outlined currently. Beyond the realm of angiosperms (and, to some
778   extent, seed plants), these regulators and their interactions have spotty data coverage, if any. The
779   presence, expression patterns, functions, and interactions of C3HDZs, SHR, SCR, miR165/166, as well as
780   auxin distribution and transport, have been slow to be explored in seed-free plants over the last 10-15
781   years, although there are notable exceptions (e.g., Floyd & Bowman 2004, 2006, 2007; Prigge & Clark
782   2006; Sanders & Langdale 2013; Frank et al. 2015; Ambrose & Vasco 2016; Vasco et al. 2016). These are
783   all important in understanding what determines stelar organization, considering that seed-free plants
784   harbor most of the diversity of stelar architecture.
785   The functions of C3HDZ genes in vascular identity and development have been confirmed, in
786   general, in many tracheophytes (Floyd & Bowman 2006; Floyd et al. 2006; Ambrose & Vasco 2016).
787   Aside from refining the functional data on C3HDZs and adding more data points (i.e., more species and
788   lineages), it will be interesting to understand if and what aspects of the development and specification
789   of boundary layers, which are ubiquitously associated with vascular tissues and the stele, share
790   regulatory mechanisms across all tracheophytes; if there is a shared specifier of the provascular domain
791   and if that key regulator is also part of the module that specifies boundary layers in all vascular plants. If
792   the same regulatory module specifying the boundary layer is shared among all living tracheophytes,
793   then this module may have evolved as early as or even before the oldest tracheophytes. If such a
794   regulatory mechanism is not shared in its entirety, then are there any components of it that are shared
795   among all tracheophytes? Answers to all these questions will help identify boundary layers in extant
796   plants even in the absence of diagnostic anatomical features and will clarify how much sense it makes to
797   use boundary layers to define and classify steles.
798   The other major direction of investigation should aim to document in detail the vascular
799   architecture and anatomy of boundary layers in as many extinct species as possible. The fossil record,
800   traditionally decried as incomplete, has offered, nevertheless, surprisingly detailed data on tissue- and
801   cell-level anatomy in multiple cases. Xylem is among the most frequently and best preserved plant
802   tissues in the fossil record and, although phloem and other "softer-walled" tissues (such as those that
803   form boundary layers) or apical meristems are preserved less frequently, continued exploration of the
804   fossil record will uncover new data on boundary layers and stelar architecture in extinct plants.
805   Although not discussed here, patterns of primary xylem maturation and the architecture of the
806   protoxylem are another aspect of plant anatomy important in understanding vascular tissue
807   differentiation and the organization of steles (Beck et al. 1982). Thus, future studies addressing these
808   aspects could illuminate in detail the relationships between protoxylem, patterns of polar auxin
809   transport, and their respective regulatory programs. Eventually, this type of data could provide answers
810   to basic questions, such as the ultimate causes of the fundamental difference in primary xylem
811   maturation between the exarch-zosterophylls and lycophytes, and the centrarch-mesarch trimerophytes
812   and euphyllophytes; or of the difference in primary xylem maturation between euphyllophytes with

813   "permanent protoxylem" (*sensu* Beck & Stein 1993) (i.e., moniliformopsids; Kenrick & Crane 1997) and

814   those with "radiate protoxylem" (radiatopsids).

References

Ambrose, B.A., Vasco, A., 2016. Bringing the multicellular fern meristem into focus. New Phytologist 210, 790–793.

Baima, S., Nobili, F., Sessa, G., et al., 1995. The expression of the *Athb-8* homeobox gene is restricted to provascular cells in *Arabidopsis thaliana*. Development 121, 4171–4182.

Banks, H. P., Leclercq, S., Hueber, F.M., 1975. Anatomy and morphology of *Psilophyton dawsonii*, sp. n. from the Late Lower Devonian of Quebec (Gaspé), and Ontario, Canada. Palaeontographica Americana 8, 75–127.

Barratt, K., 1920. A contribution to our knowledge of the vascular system of the genus *Equisetum*. Annals of Botany 34, 201–235.

Beck, C.B., 197. The appearance of the gymnospermous structure. Biological Reviews 45, 379–400.

Beck, C.B., 1971. On the anatomy and morphology of lateral branch systems of *Archaeopteris*. American Journal of Botany 58, 758–784.

Beck, C.B., 1976. Current status of the Progymnospermopsida. Review of Palaeobotany and Palynology 21, 5–23.

Beck, C.B., 1979. The primary vascular system of *Callixylon*. Review of Palaeobotany and Palynology 28, 103–115.

Beck, C.B., Stein, W.E., 1993. *Crossia virginiana* gen. et sp. nov., a new member of the Stenokoleales from the Middle Devonian of southwestern Virginia. Palaeontographica B 229, 115–134.

Beck, C.B., Schmid, R., Rothwell, G.W., 1982. Stelar morphology and the primary vascular system of seed plants. Botanical Review 48, 691–815, 913–931.

Benzing, D.H., 1967a. Developmental patterns in stem primary xylem of woody Ranales. I. Species with unilacunar nodes. American Journal of Botany 54, 805–813.

Benzing, D.H., 1967b. Developmental patterns in stem primary xylem of woody Ranales. II. Species with trilacunar and multilacunar nodes. American Journal of Botany 54, 813–820.

Bertrand, P., 1935. Contribution à l'étude des cladoxylées de Saalfeld. Palaeontographica B 80, 101–179.

Bickner, M.A., Tomescu, A.M.F., 2019. Structurally complex, yet anatomically plesiomorphic: permineralized plants from the Emsian of Gaspé (Quebec, Canada) expand the diversity of Early Devonian euphyllophytes. IAWA Journal 40, doi: 10.1163/22941932-40190234

Bierhorst, D.W., 1971. Morphology of vascular plants. Macmillan, New York.

Boodle, L.A., 1901. Comparative anatomy of the Hymenophyllaceae, Schizaeaceae, and Gleicheniaceae. II. On the anatomy of the Schizaeaceae. Annals of Botany 15, 359–421.

Bower, F.O., 1908. The origin of a land flora. A theory based upon the facts of alternation. Macmillan, London.

Bower, F.O., 1923. The ferns (Filicales) treated comparatively with a view to their natural classification. Vol. 1, Analytical examination of the criteria of comparison. Cambridge University Press, Cambridge, UK.

Boyce, C.K., 2008. How green was *Cooksonia*? The importance of size in understanding the early evolution of physiology in the vascular plant lineage. Paleobiology 34, 179–194.

Brebner, G., 1902. On the anatomy of *Danaea* and other Marattiaceae. Annals of Botany 16, 517–552.

Caggiano, M.P., Yu, X., Bhatia, N., et al., 2017. Cell type boundaries organize plant development. eLife 6, e27421.

Campbell, L., Turner, S., 2017. Regulation of vascular cell division. Journal of Experimental Botany 68, 27–43.

Carlsbecker, A., Lee, J.-Y., Roberts, C.J., et al., 2010. Cell signalling by microRNA165/6 directs gene dose-dependent root cell fate. Nature 465, 316–321.

Carluccio, L.M., Hueber, F.M., Banks, H.P., 1966. *Archaeopteris macilenta*, anatomy and morphlogy of its frond. American Journal of Botany 53, 719–730.

863   Cascales-Miñana, B., Steemans, P., Servais, T., et al., 2019. An alternative model for the earliest
864   evolution of vascular plants. Lethaia 52, doi: 10.1111/let.12323.
865   Cronk, Q.C.B., 2009. The molecular organography of plants. Oxford University Press, Oxford, UK.
866   Cui, H., Levesque, M.P., Vernoux, T., et al., 2007. An evolutionarily conserved mechanism delimiting SHR
867   movement defines a single layer of endodermis in plants. Science 316, 421–425.
868   de Luis Balaguer, M.A., Fisher, A.P., Clark, N.M., et al., 2017. Predicting gene regulatory networks by
869   combining spatial and temporal gene expression data in *Arabidopsis* root stem cells. Proceedings
870   of the National Academy of Sciences USA 114, E7632–E7640.
871   Decombeix, A.-L., Boura, A., Tomescu, A.M.F., 2019. Plant hydraulic architecture through time: lessons
872   and questions on the evolution of vascular systems. IAWA Journal 40, doi: 10.1163/22941932-
873   40190254
874   Delevoryas, T., 1964. Ontogenetic studies of fossil plants. Phytomorphology 14, 299–314.
875   Dennis, R.L., 1974. Studies of Paleozoic ferns: *Zygopteris* from the Middle and Late Pennsylvanian of the
876   United States. Palaeontographica B 148, 95–136.
877   Di Laurentio, L., Wysocka-Diller, J.W., Malamy, J.E., et al., 1996. The *SCARECROW* gene regulates an
878   asymmetric cell division that is essential for generating the radial organization of the *Arabidopsis*
879   root. Cell 86, 423–433.
880   Donner, T.J., Scarpella, E., 2009. Auxin-transport-dependent leaf vein formation. Botany 87, 678–684.
881   Drapek, C., Sparks, E.E., Marhavy, P., et al., 2018. Minimum requirements for changing and maintaining
882   endodermis cell identity in the *Arabidopsis* root. Nature Plants 4, 586–595.
883   Edwards, D., 1970. Further observations on the Lower Devonian plant, *Gosslingia breconensis* Heard.
884   Philosophical Transactions of the Royal Society of London B 258, 225–243.
885   Edwards, D., 1981. Studies on Lower Devonian petrifactions from Britain. 2. *Sennicaulis*, a new form
886   genus for sterile axes based on pyrite and limonite petrifactions from the Senni beds. Review of
887   Palaeobotany and Palynology 32, 207–226.
888   Edwards, D., 1994. Toward an understanding of pattern and process in the growth of early vascular
889   plants. In: Ingram, D.D., Hudson, A. (Eds.), Shape and Form in Plants and Fungi. London: Academic
890   Press/Linnean Society of London, pp. 39–59.
891   Edwards, D., Davies, K.L., Axe, L. 1992. A vascular conducting strand in the early land plant *Cooksonia*.
892   Nature 357, 683–685.
893   Eggert, D.A., 1961. The ontogeny of Carboniferous arborescent Lycopsida. Palaeontographica B 108, 43–
894   92.
895   Esau, K., 1965. Plant anatomy. Second edition. Wiley, New York.
896   Esau, K., 1977. Anatomy of seed plants. Second edition. Wiley, New York.
897   Farmer, J.B., Hill, T.G., 1902. On the arrangement and structure of the vascular strands in *Angiopteris*
898   *evecta*, and some other Marattiaceae. Annals of Botany 16, 371–402.
899   Floyd, S.K., Bowman, J.L., 2004. Ancient microRNA target sequences in plants. Nature 428, 485–486.
900   Floyd, S.K., Bowman, J.L., 2006. Distinct developmental mechanisms reflect the independent origins of
901   leaves in vascular plants. Current Biology 16, 1911–1917.
902   Floyd, S.K., Bowman, J.L., 2007. The ancestral developmental tool kit of land plants. International Journal
903   of Plant Sciences 168, 1–35.
904   Floyd, S.K., Bowman, J.L., 2010. Gene expression patterns in seed plant shoot meristems and leaves:
905   homoplasy or homology? Journal of Plant Research 123, 43–55.
906   Floyd, S.K., Zalewski, C.S., Bowman, J.L., 2006. Evolution of class III Homeodomain-leucine zipper genes
907   in streptophytes. Genetics 173, 373–388.
908   Frank, M.H., Edwards, M.B., Schultz, E.R., et al., 2015. Dissecting the molecular signatures of apical cell-
909   type shoot meristems from two ancient land plant lineages. New Phytologist 207, 893–904.

910   Fukaki, H., Wysocka-Diller, J.W., Kato, T., et al., 1998. Genetic evidence that the endodermis is essential
911   for shoot gravitropism in *Arabidopsis thaliana*. Plant Journal 14, 425–430.
912   Gardiner, J., Donner, T.J., Scarpella, E., 2011. Simultaneous activation of *SHR* and *ATHB8* expression
913   defines switch to preprocambial cell state in *Arabidopsis* leaf development. Developmental
914   Dynamics 240, 261–270.
915   Gensel, P.G., 1976. *Renalia hueberi*, a new plant from the Lower Devonian of Gaspé. Review of
916   Palaeobotany and Palynology 22, 19–37.
917   Gensel, P.G., 1984. A new Lower Devonian plant and the early evolution of leaves. Nature 309, 785–787.
918   Gola, E.M., Jernstedt, J.A., Zagorska-Marek, B., 2007. Vascular architecture in shoots of early divergent
919   vascular plants, *Lycopodium clavatum* and *Lycopodium annotinum*. New Phytologist 174, 774–786.
920   Good, C.W., Taylor, T.N., 1972. The ontogeny of Carboniferous articulates: the apex of *Sphenophyllum*.
921   American Journal of Botany 59, 617–626.
922   Gwynne-Vaughn, D.T., 1901. Observations on the anatomy of solenostelic ferns. I. *Loxsoma*. Annals of
923   Botany 15, 71–98.
924   Hébant, C., 1977. The conducting tissues of bryophytes. J. Cramer, Vaduz.
925   Helariutta, Y., Fukaki, H., Wysocka-Diller, J.W., et al., 2000. The *SHORT-ROOT* gene conrols radial
926   patterning of the *Arabidopsis* root through radial signalling. Cell 101, 555–567.
927   Hetherington, A.J., Dubrovski, J.G., Dolan, L., 2016. Unique cellular organisation in the oldest root
928   meristem. Current Biology 26, 1629–1633.
929   Hetherington, A.J., Dolan, L., 2018. Rhynie chert fossils demonstrate the independent origin and gradual
930   evolution of lycophyte roots. Current Opinion in Plant Biology 47, 119–126.
931   Hisanaga, T., Miyashima, S., Nakajima, K., 2014. Small RNAs as positional signal for pattern formation.
932   Current Opinion in Plant Biology 21, 37–42.
933   Ilegems, M., Douet, V., Meylan-Bettex, M., et al., 2010. Interplay of auxin, KANADI and Class III HD-ZIP
934   transcription factors in vascular tissue formation. Development 137, 975–984.
935   Jeffrey, E.C., 1899. The morphology of the central cylinder in the angiosperms. Transactions of the Royal
936   Canadian Institute 6, 599–636.
937   Juarez, M.T., Kui, J.S., Thomas, J., et al., 2004. microRNA-mediated repression of *rolled leaf1* specifies
938   maize leaf polarity. Nature 428, 84–88.
939   Karafit, S.J., Rothwell, G.W., Stockey, R.A., Nishida H., 2006. Evidence for sympodial vascular architecture
940   in a filicalean fern rhizome: *Dickwhitea allenbyensis* gen. et sp. nov. (Athyriaceae). International
941   Journal of Plant Sciences 167, 721–727.
942   Kenrick, P., Crane, P.R., 1997. The origin and early diversification of land plants. Smithsonian Institution
943   Press, Washington D.C., USA.
944   Kidston, R., Gwynne-Vaughan, D.T., 1914. On the fossil Osmundaceae. Part V. Transations of the Royal
945   Society of Edinburgh 50, 469–480.
946   Kidston, R., Lang, W.H., 1917. On Old Red Sandstone plants showing structure from the Rhynie Chert
947   Bed, Aberdeenshire. Part 1. *Rhynia gwynne-vaughani* Kidston and Lang. Transactions of the Royal
948   Society of Edinburgh 51, 751–784.
949   Kidston, R., Lang, W.H., 1920a. On Old Red Sandstone plants showing structure, from the Rhynie Chert
950   Bed, Aberdeenshire. Part II. Additional notes on *Rhynia gwynne-vaughani*, Kidston and Lang; with
951   descriptions of *Rhynia major*, n. sp., and *Hornea lignieri*, n. g., n. sp. Transactions of the Royal
952   Society of Edinburgh 52, 603–627.
953   Kidston, R., Lang, W.H., 1920b. On Old Red Sandstone plants showing structure, from the Rhynie Chert
954   Bed, Aberdeenshire. Part III. *Asteroxylon mackiei*, Kidston and Lang. Transactions of the Royal
955   Society of Edinburgh 52, 643–680.
956   Leclercq, S., Banks, H.P., 1962. *Pseudosporochnus nodosus* sp. nov., a Middle Devonian plant with
957   cladoxylalean affinities. Palaeontographica B 110, 1–34.

958   Levesque, M.P., Vernoux, T., Busch, W., et al., 2006. Whole-genome analysis of the SHORT-ROOT
959   developmental pathway in *Arabidopsis*. PLoS Biology 4, e 143.
960   Ma, Y., Steeves, T.A., 1992. Auxin effects on vascular differentiation in ostrich fern. Annals of Botany 70,
961   277–282.
962   Ma, Y., Steeves, T.A., 1995. Effects of developing leaves on stelar pattern development in the shoot apex
963   of *Matteuccia struthiopteris*. Annals of Botany 75, 593–603.
964   Matsunaga, K.K.S., Tomescu, A.M.F., 2017. An organismal concept for *Sengelia radicans* gen. et sp. nov.
965   – morphology and natural history of an Early Devonian lycophyte. Annals of Botany 119, 1097–
966   1113.
967   Matten, L.C., 1968. *Actinoxylon banksii* gen. et sp. nov.: a progymnosperm from the Middle Devonian of
968   New York. American Journal of Botany 55, 773–782.
969   Mattsson, J., Ckurshumova, W., Berleth, T., 2003. Auxin signaling in *Arabidopsis* leaf vascular
970   development. Plant Physiology 131, 1327–1339.
971   Melchior, R.C., Hall, J.W., 1961. A calamitean shoot apex from the Pennsylvanian of Iowa. American
972   Journal of Botany 48, 811–815.
973   Miller, C.N.J., 1971. Evolution of the fern family Osmundaceae based on anatomical studies.
974   Contributions from the Museum of Paleontology, University of Michigan 23, 105–169.
975   Miyashima, S., Koi, S., Hashimoto, T., Nakajima, K., 2011. Non-cell-autonomous microRNA165 acts in a
976   dosedependent manner to regulate multiple differentiation status in the *Arabidopsis* root.
977   Development 138, 2303–2313.
978   Muraro, D., Mellor, N., Pound, M.P., et al., 2014. Integration of hormonal signaling networks and mobile
979   microRNAs is required for vascular patterning in *Arabidopsis* roots. Proceedings of the National
980   Academy of Sciences USA 111, 857–862.
981   Namboodiri, K.K., Beck, C.B., 1968. A comparative study of the primary vascular system of conifers. III.
982   Stelar evolution in gymnosperms. American Journal of Botany 55, 464–472.
983   Ogura, Y., 1972. Comparative anatomy of vegetative organs of the pteridophytes. Gebruder
984   Borntraeger, Berlin.
985   Prigge, M.J., Clark, S.E., 2006. Evolution of the class III HD-Zip gene family in land plants. Evolution and
986   Development 8, 350–361.
987   Posthumus, O., 1924. On some principles of stelar morphology. De Bussy, Amsterdam.
988   Ramachandran, P., Carlsbecker, A., Etchells, J.P., 2017. Class III HD-ZIPs govern vascular cell fate: an HD
989   view on patterning and differentiation. Journal of Experimental Botany 68, 55–69.
990   Reinhardt, D., 2005. Phyllotaxis - a new chapter in an old story about beauty and magic numbers.
991   Current Opinion in Plant Biology 8, 487–493.
992   Remy W., Hass H., 1986. *Gothanophyton zimmermannii* nov. gen. nov. spec., eine Pflanze mit
993   komplexem stellar Körper aus dem Emsium. Argumenta Palaeobotanica 7, 9–69.
994   Rothwell, G.W., 1976. Primary vasculature and gymnosperm systematics. Review of Palaeobotany and
995   Palynology 22, 193–206.
996   Rothwell, G.W., 1992. The evolution of vascular architecture. [unpublished; see Appendix]
997   Rothwell, G.W., Erwin, D.M., 1987. Origin of seed plants: an aneurophyte/seed-fern link elaborated.
998   American Journal of Botany 74, 970–973.
999   Sanchez, P., Nehlin, L., Greb, T., 2012. From thin to thick: major transitions during stem development.
1000   Trends in Plant Science 17, 113–121.
1001   Sanders, H.L., Langdale, J.A., 2013. Conserved transport mechanisms but distinct auxin responses govern
1002   shoot patterning in *Selaginella kraussiana*. New Phytologist 198, 419–428.
1003   Scarpella, E., Rueb, S., Boot, K.J.M., et al., 2000. A role for the rice homeobox gene *Oshox1* in
1004   provascular cell fate commitment. Development 127, 3655–3669.

Scheckler, S.E., 1978. Ontogeny of progymnosperms. II. Shoots of Upper Devonian Archaeopteridales. Canadian Journal of Botany 56, 3136–3170.

Schmid, R., 1982. The terminology and classification of steles. Botanical Review 48, 817–931.

Schoute, J.C., 1903. Die Stelär-Theorie. Gustav Fischer, Jena, Germany.

Scott, D.H., 1902. Professor Jeffrey's theory of the stele. New Phytologist 1, 207–212.

Serbet, R., Rothwell, G.W., 1992. Characterizing the most primitive seed ferns. I. A reconstruction of *Elkinsia polymorpha*. International Journal of Plant Sciences 153, 602–521.

Siebers, A.M., 1971. Initiation of radial polarity in the interfascicular cambium of *Ricinus communis* L. Acta Botanica Neerlandica 20, 211–220.

Slater, B.J., McLoughlin, S., Hilton, J., 2015. A high-latitude Gondwanan lagerstätte: The Permian permineralised peat biota of the Prince Charles Mountains, Antarctica. Gondwana Research 27, 1446–1473.

Soe, K., 1959. Morphogenetic studies on *Onoclea sensibilis* L. Ph. D. thesis, Harvard University, Cambridge, USA.

Soria, A., Meyer-Berthaud, B., 2003. Occurrence of whorled organotaxis in the cladoxylopsid *Pietzschia polyupsilon* Read and Campbell. Review of Palaeobotany and Palynology 124, 29–49.

Stein, W.E., 1993. Modeling the evolution of stelar architecture in vascular plants. International Journal of Plant Sciences 154, 229–263.

Stewart, W.N., Rothwell, G.W., 1993. Paleobotany and the evolution of plants. Second edition. Cambridge University Press, Cambridge, UK.

Strullu-Derrien, C., Kenrick, P., Tafforeau, P., et al., 2014. The earliest fossil wood and its hydraulic properties documented in *c.* 407-million-year-old fossils using synchrotron microtomography. Botanical Journal of the Linnean Society 175, 423–437.

Tansley, A.G., 1896. The stelar theory; a history and a criticism. Science Progress 5, 133–150, 215–226.

Tansley, A.G., 1907. Lectures on the evolution of the filicinean vascular system. New Phytologist 6, 25–35, 53–68, 109–120, 135–147, 148–155, 187–203, 219–238, 253–269.

Tansley, A.G., 1908. Lectures on the evolution of the filicinean vascular system. New Phytologist 7, 1–16, 29–40.

Toledo, S., Bippus, A.C., Tomescu, A.M.F., 2018. Buried deep beyond the veil of extinction: euphyllophyte relationships at the base of the spermatophyte clade. American Journal of Botany 105, 1264–1285.

Tomescu, A.M.F., 2008. The endodermis: a horsetail's tale. New Phytologist 177, 291–295.

Tomescu, A.M.F., 2009. Megaphylls, microphylls and the evolution of leaf development. Trends in Plant Science 14, 5–12.

Tomescu, A.M.F., Escapa, I.H., Rothwell, G.W., et al., 2017. Developmental programmes in the evolution of *Equisetum* reproductive morphology: a hierarchical modularity hypothesis. Annals of Botany 119, 489–505.

Troop, J.E., Mickel, J.T., 1968. Petiolar shoots in the Dennstaedtioid and related ferns. American Fern Journal 58, 64–70.

Unger, F., 1856. Schiefer- und Sandsteinflora. Denkschriften der Kaiserlichen Akademie der Wissenschaften zu Wien. Mathematisch-Naturwissenschaftliche Classe 11, 139–182.

Van Fleet, D.S., 1950. The cell forms, and their common substance reactions, in the parenchyma-vascular boundary. Bulletin of the Torrey Botanical Club 77, 340–353.

Van Fleet, D.S., 1961. Histochemistry and function of the endodermis. Botanical Review 27, 165–220.

van Tieghem, P., Douliot, H., 1886a. Sur les tiges à plusieurs cylindres centraux. Bulletin de la Société Botanique de France 33, 213–216.

van Tieghem, P., Douliot, H., 1886b. Sur la polystélie. Annales des Sciences Naturelles, Botanique, Série 7, 3, 275–322.

1053   Vasco, A., Smalls, T.L., Graham, S.W., et al., 2016. Challenging the paradigms of leaf evolution: class III
1054   HD-Zips in ferns and lycophytes. New Phytologist 212, 745–758.
1055   Wang, H., Avci, U., Nakashima, J., et al., 2010. Mutation of WRKY transcription factors initiates pith
1056   secondary wall formation and increases stem biomass in dicotyledonous plants. Proceedings of
1057   the National Academy of Sciences USA 107, 22338–22343.
1058   Wardlaw, C.W., 1946. Experimental and analytical studies of pteridophytes. VII. Stelar morphology: the
1059   effect of defoliation on the stele of *Osmunda* and *Todea*. Annals of Botany 9, 97–107.
1060   White, R.A., Weidlich, W.H., 1995. Organization of the vascular system in the stems of *Diplazium* and
1061   *Blechnum* (Filicales). American Journal of Botany 82, 982–991.
1062   Wight, D.C., 1987. Non-adaptive change in early land plant evolution. Paleobiology 13, 208–214.
1063   Williams, S., 1927. A critical examination of the Vittarieae with a view to their systematic comparison.
1064   Transactions of the Royal Society of Edinburgh 55, 173–217.
1065   Wysocka-Diller, J.W., Helariutta, Y., Fukaki, H., et al., 2000. Molecular analysis of SCARECROW function
1066   reveals a radial patterning mechanism common to root and shoot. Development 127, 595–603.
1067   Xu, H.-H., Berry, C.M., Stein, W.E., et al., 2017. Unique growth strategy in the Earth's first trees revealed
1068   in silicified fossil trunks from China. Proceedings of the National Academy of Sciences USA 114,
1069   12009–12014.

1070   **Figures**
1071
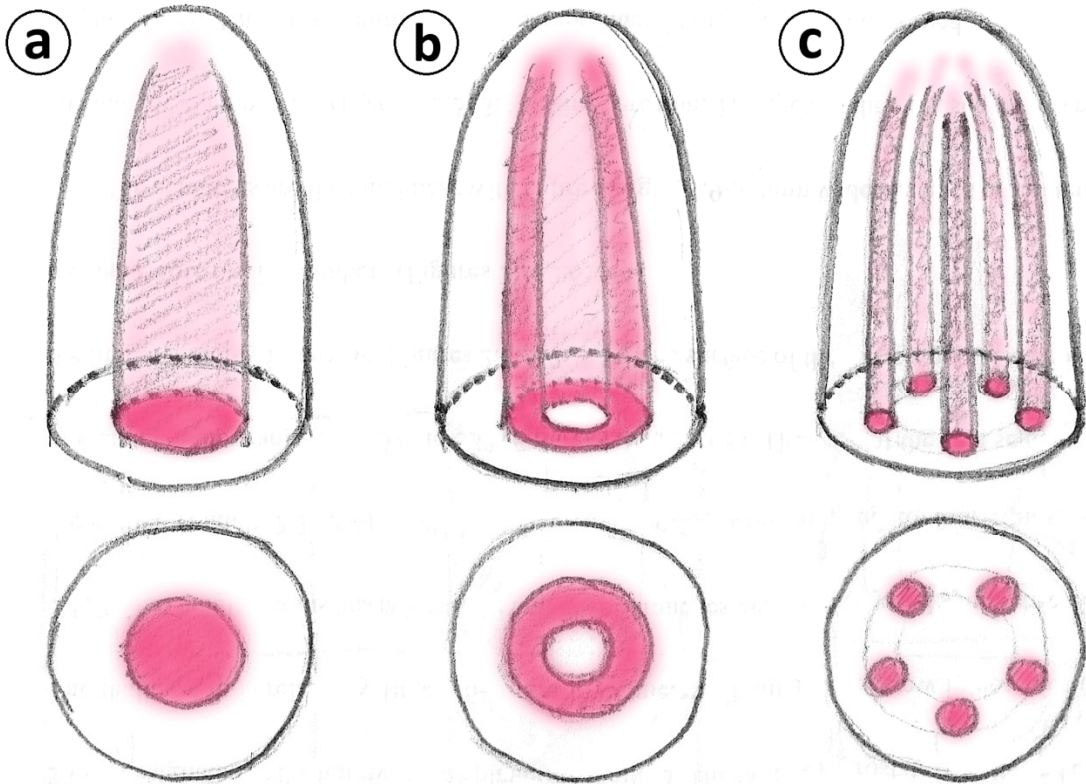
1072
1073
1074   **Figure 1.** The geometry of the procambium (pink/red) in the apical meristem region (top panel)
1075   provides a criterion for defining three main types of stele (seen in cross section in the bottom panel). A
1076   protostele (**a**) is a stele derived from a solid central strand of procambium. The procambium is
1077   surrounded by ground meristem that matures into the cortex. A siphonostele (**b**) develops from a
1078   hollow cylinder of procambium. Aside from ground meristem that differentiates into the cortex that
1079   surrounds the stele, siphonostelic axes possess a central cylinder of ground meristem that forms the
1080   mature pith. A eustele (**c**) is a stele derived from a number of discrete procambial strands that, taken
1081   together, describe a more-or-less circular outline in cross sections, separating an outer cortex and a
1082   central pith, both derived from ground meristem. The parenchymatous areas between adjacent
1083   vascular strands are interfascicular areas (also termed pith rays).
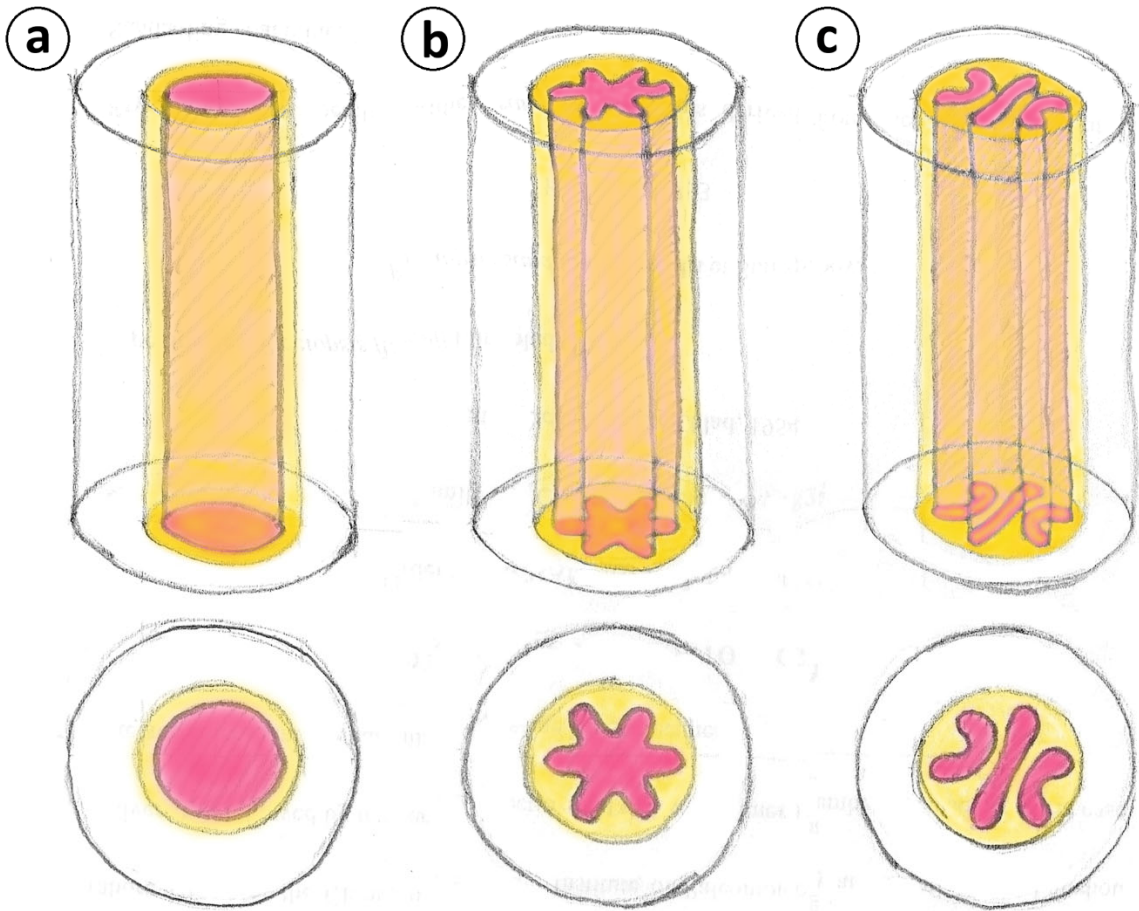
1084
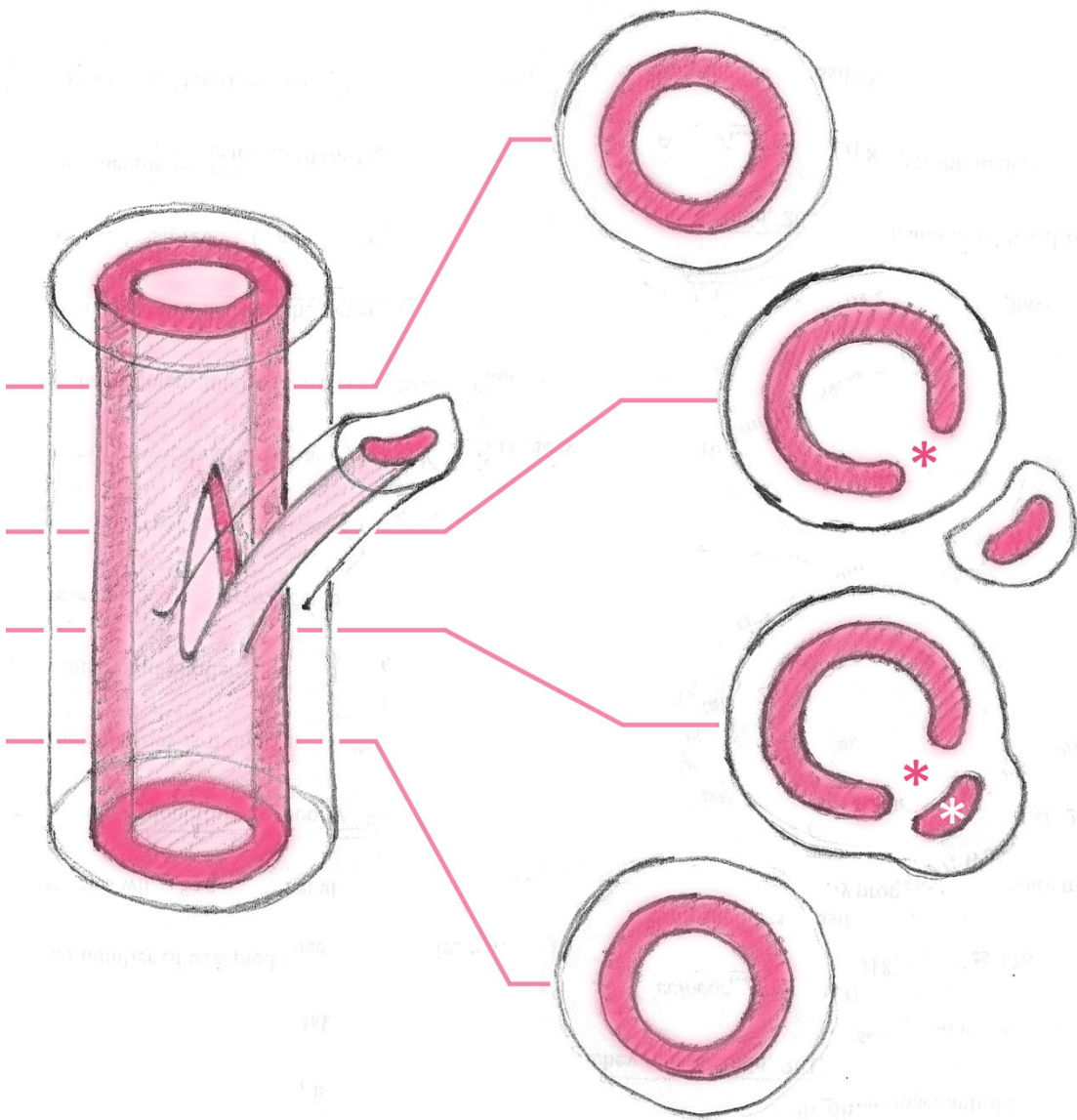
1085
1086
1087   **Figure 2.** The leaf gap (pink asterisk) produced in a siphonostele by the divergence of a vascular trace
1088   supplying the base of a leaf (leaf trace; white asterisk); tissues of the stele and leaf trace shown in
1089   pink/red.

1090

1091
1092
1093   **Figure 3.** Protosteles (top panel) are divided, based on the cross-sectional geometry of the primary
1094   xylem (bottom panel) into haplosteles, wherein the xylem has circular to oval shape in cross section (**a**),
1095   actinosteles, wherein the xylem has has a lobed (ribbed) shape (**b**), and plectosteles, with the xylem
1096   irregularly dissected into lobes and bands (**c**); xylem shown in red and additional stele tissues in yellow;
1097   the endodermis, not depicted, follows the boundary between the yellow tissues of the stele and the
1098   white tissues of the cortex.

1099
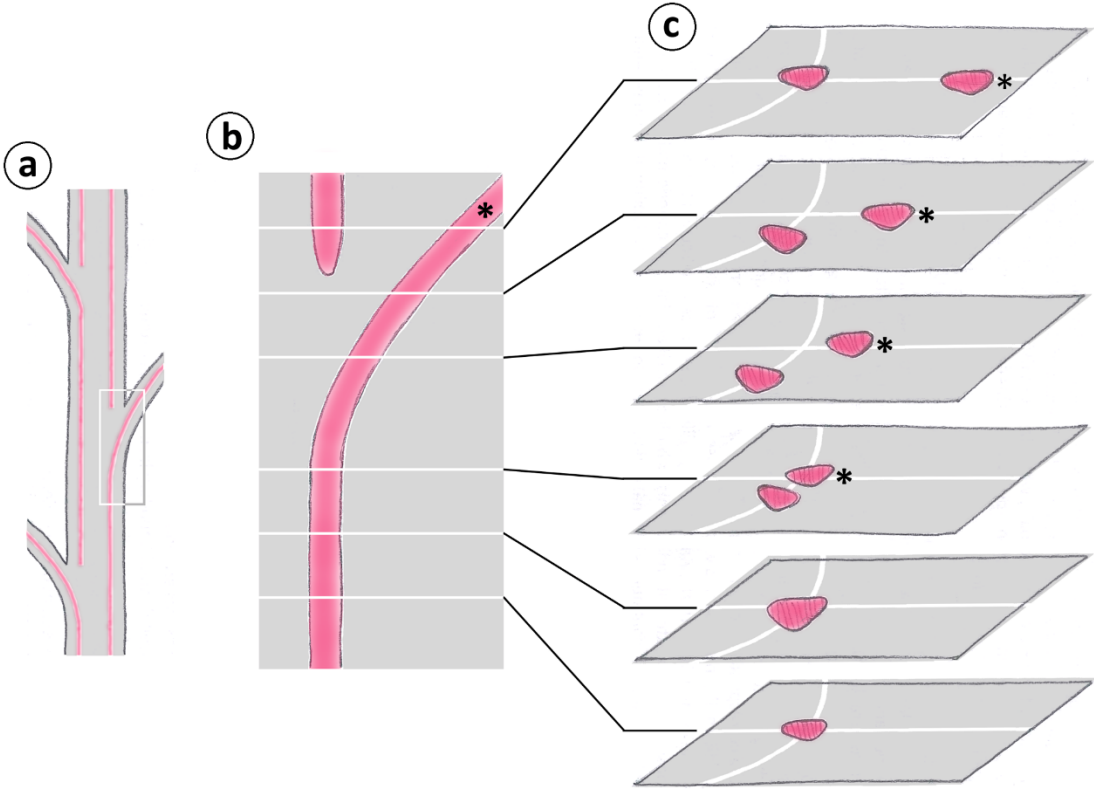
1100
1101
1102   **Figure 4.** Longitudinal sections through eustelic axes often show vascular tissue configurations that look
1103   misleadingly like leaf gaps (**a, b**). In the vicinity of the shoot apical meristem this configuration is due to
1104   the fact that nodal tissues mature earlier than those of the internodes, thus, a procambial strand that is
1105   conspicuous in a node can appear to lose its substance along its trajectory through the internode below,
1106   and to reappear in the next node underneath. In the mature shoot portions of most seed plants, leaf
1107   traces (asterisk) diverge from cauline bundles in a tangential direction (**c**, bottom three planes of
1108   section) before traversing the cortex in a radial direction and upwards (**c**, top three planes of section).
1109   This leads to tangential displacement of the cauline bundle above the divergence (**c**), as a result of which
1110   the bundle shows a hiatus immediately above the node in longitudinal sections (**b**), similar to that
1111   produced by a leaf gap in a siphonostele longitudinal section.

1112
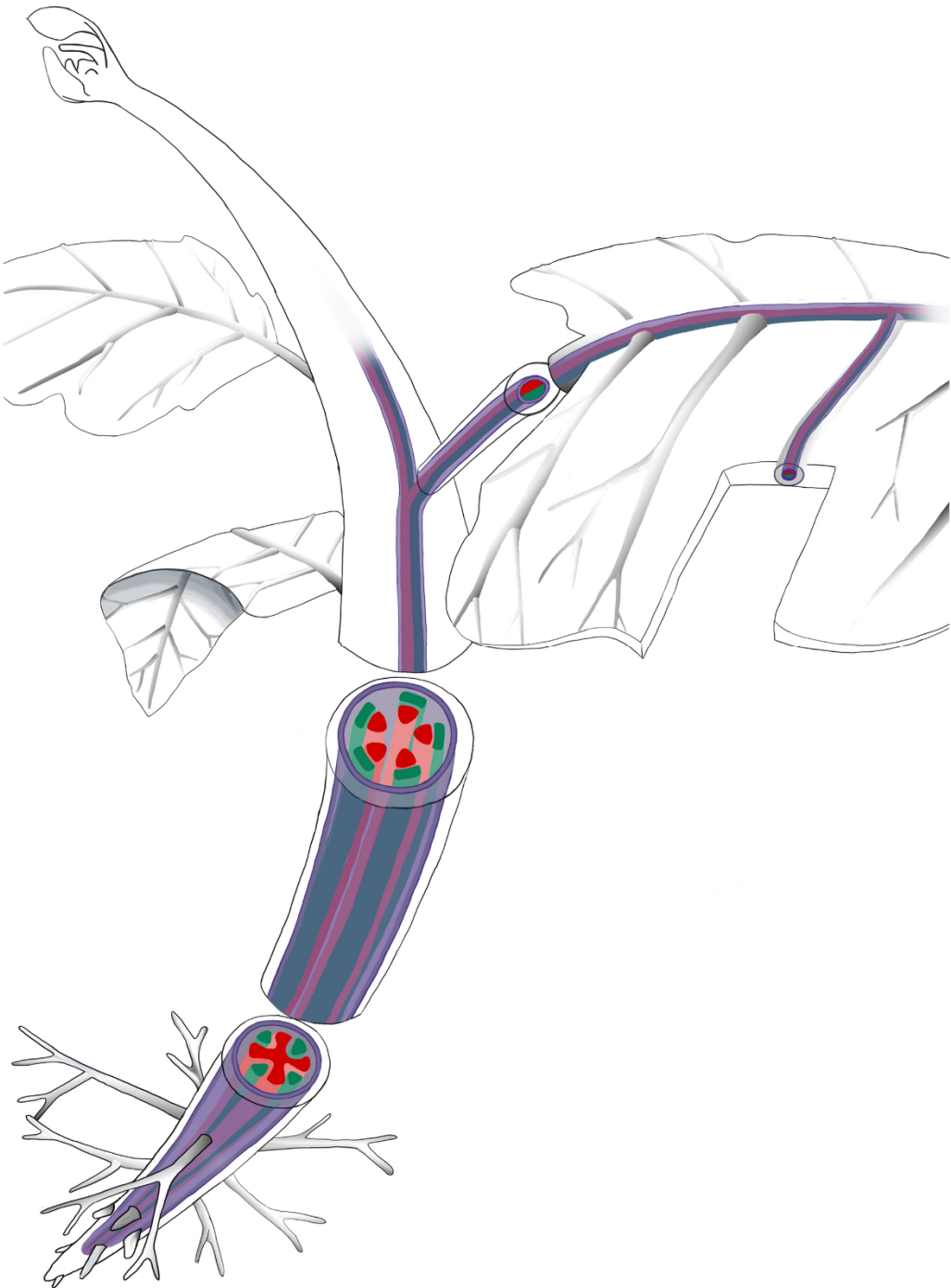
1113
1114
1115   **Figure 5**. The layers that mark boundaries between the vascular tissues (primary xylem in red and
1116   primary phloem in green) and ground tissues. These layers – the endodermis in roots, the starch sheath
1117   in stems, and the bundle sheaths of leaf veins (all shown in purple) – are continuous throughout the
1118   plant body, despite having distinct physiological functions, and the available evidence suggests that they
1119   are specified by the same regulatory modules throughout the plant body. Artwork by Danza Chisholm-
1120   Sims.

1121
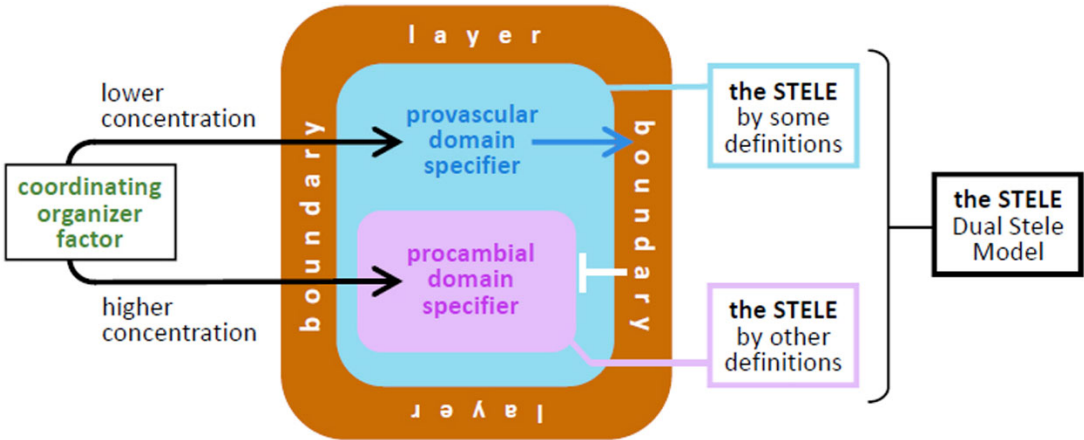
1122
1123
1124   **Figure 6**. The stele has been defined traditionally as comprising either the tissues derived from
1125   procambium or the tissues contained within a boundary layer. The *dual stele model* provides a unifying
1126   explanation for the nature and evolution of the stele, consistent with both the procambial and the
1127   boundary layer views. This model posits two cell fate specification mechanisms that are deployed
1128   sequentially and delimit increasingly more narrowly circumscribed and more specialized developmental
1129   domains. The first mechanism (i) specifies a provascular domain (blue), wherein cells maintain
1130   competency to differentiate into procambial tissue, and (ii) establishes (blue arrow) a boundary layer
1131   (brown) that separates this domain from the neighboring accessory domain. The second mechanism
1132   specifies procambial identity (pink) in cells within the provascular domain that will differentiate into
1133   xylem and phloem. The two cell fate specification mechanisms that determine the provascular and
1134   procambial domains are connected through the intermediary of the boundary layer, which inhibits the
1135   activity of the procambial domain specifier (white inhibitory interaction symbol), thus constraining the
1136   physical extent of this domain. The two mechanisms are also coordinated by an organizer factor that
1137   acts in a dosage-dependent manner: promoting the provascular domain specifier at lower
1138   concentrations and the procambial domain specifier at higher concentrations. Current understanding of
1139   developmental regulation in stele tissues and boundary layers suggests that auxin may be the
1140   coordinating organizer factor, with SHR (homologs) and class III HD-Zip genes (C3HDZ) the provascular
1141   and procambial domain specifiers, respectively. SHR is known to act in specification of the boundary
1142   layer and in activation, within this layer, of miR165/166, which diffuse back into the provascular domain,
1143   inhibiting the activity of C3HDZ and constraining the extent of the procambial domain.

1144
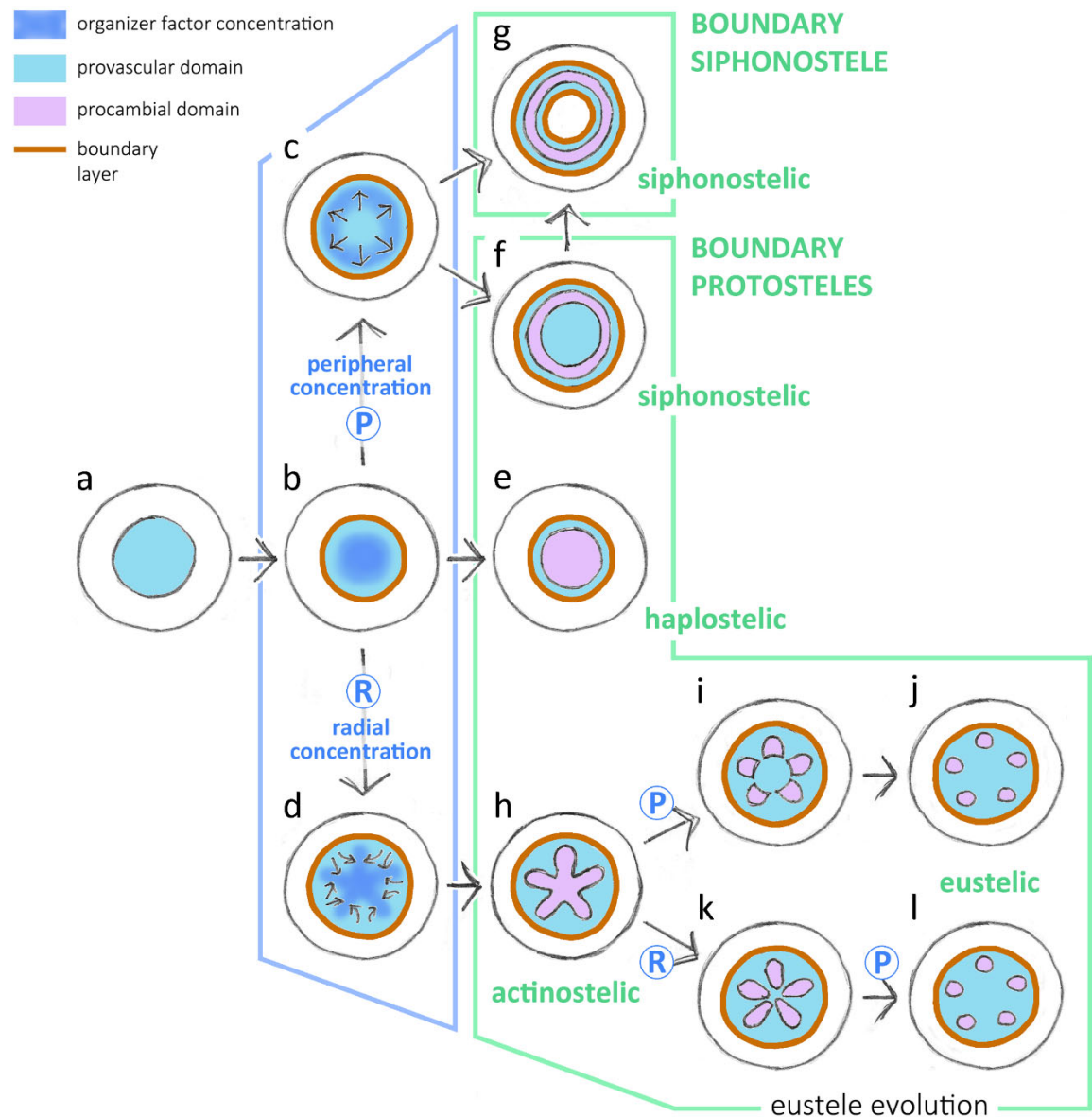
1145
1146
1147 **Figure 7**. Stele types in an evolutionary-developmental perspective informed by the dual stele model. A
1148 central column of tissue with provascular identity (light blue) and the boundary layer (brown) that it
1149 establishes at its periphery (**a → b**) define a central domain, corresponding to the stele, and an outer
1150 (accessory) domain. This type of general organization is termed a **boundary protostele** in the
1151 classification proposed here. Within the provascular domain, a central zone of higher concentration
1152 (dark blue) of the organizer factor (auxin) specifies a strand of procambial domain (pink) with terete
1153 geometry (**b → e**), as seen in protosteles of the haplostele type (**e**; *haplostelic boundary protostele*).
1154 Peripheral redistribution (P) of organizer factor concentrations (**b → c**) specifies a procambial domain in
1155 the shape of a hollow cylinder typical of siphonostelic organization (**f**; *siphonostelic boundary*
1156 *protostele*). A marked depletion in organizer factor at the center of the stele leads to specification of a
1157 second boundary layer and to a provascular domain shaped like a hollow cylinder; in the classification
1158 proposed here, this organization is termed a **boundary siphonostele** (**g**). Evolutionary transitions
1159 between the two types of siphonostelic organization (**f → g**) may be at the origin of the boundary

1160   siphonosteles known in some plant groups. Radial redistribution (R) of organizer factor concentrations
1161   (**b → d**) specifies a central procambial domain with vertical ridges and grooves (**d → h**), as seen in
1162   protosteles of the actinostele type (**h**; *actinostelic boundary protostele*). From such actinostelic
1163   configurations, steles with eustelic organization, i.e., procambial domain forming discrete strands (**j, l**;
1164   *eustelic boundary protostele*) could have evolved along two pathways: one emphasizing subsequent
1165   peripheral concentration (P) and referred to as medullation (**h → i → j**); and the other emphasizing
1166   further radial concetration (R) followed by peripheral concentration (P) and referred to as dissection or
1167   fragmentation (**h → k → l**). Stele color coding: boundary layer – brown line; provascular domain – light
1168   blue; procambial domain – pink; concentration of organizing factor (auxin) within the provascular
1169   domain – dark blue. Blue box – Patterns of organizing factor concentration; green boxes – classification
1170   of steles proposed here. Traditional stele types: haplostele (protostele) – **e**; actinostele (protostele) – **h**;
1171   medullated protostele and ectophloic siphonostele – **f**; amphiphloic siphonostele – **g**; eustele – **j**, **l**.

1172

1173
1174
1175   **Figure 8**. Development of the stele with double endodermis in an *Equisetum* shoot. Growth arises from
1176   the activity of (i) an apical meristem (represented by the apical cell of the shoot at left) that lays down a
1177   stack of phytomers (the first six are marked by the gray bars at far left), and (ii) intercalary meristems
1178   that are located basally in each phytomer wherein fuel internode elongation. A hypothetical
1179   developmental sequence involves several stages (labeled 1 through 5 and mapped on the shoot at left):
1180   initial specification of a central provascular domain within young phytomers (1) in early stages of radial
1181   patterning; subsequent peripheral concentration leading to a hollow cylinder of provascular domain (2);
1182   specification of inner and outer endodermal layers (3) in the upper nodal tier of a phytomer, as this tier
1183   starts differentiating from the lower internode tier (dashed line); procambial domain specification (4) in
1184   the nodal tier, between the two endodermal layers, while the internode tier remains meristematic
1185   (green in the shoot at left), forming an intercalary meristem; in growing internodes (e.g., basal-most
1186   phytomer in the shoot at left), acroscopic production of new tissue by the intercalary meristem at high
1187   rates and fast internode elongation maintain low levels of auxin in the provascular domain, precluding
1188   specification of procambial domain between the two endodermal layers (3); procambial strands
1189   differentiate within the provascular domain of the internode (5) along vertical lines corresponding to,
1190   and under the influence of, leaf primordia.

Appendix
Gar W. Rothwell's "The evolution of vascular architecture"
Extended abstract of paper presented in the Katherine Esau International Symposium "Plant structure: concepts, connections, and challenges", March 28-31, 1992, University of California, Davis, USA

The Evolution of Vascular Architecture

Gar W. Rothwell

Department of Botany, Ohio University, Athens, OH, 45701

Vascular tissues are the focus of considerable attention across a broad spectrum of botanical inquiry. Undoubtedly, this reflects the functional, developmental and phylogenetic significance of this most intricate of all plant tissue systems. While there is a relative consistency to the polyarch, exarch actinosteles found in most true roots, there is a broad spectrum of systematically and functionally correlated variation in the vascular architecture of shoot systems.

Traditional studies have, during different periods of time, emphasized divergent facets of vascular architecture. Some of the earliest studies characterized the courses of individual bundles as they traversed stems and diverged to leaves. With the formulation of the stelar theory, emphasis shifted to the overall pattern of vascular tissues in the stem. This approach has demonstrated systematic correlations among shoot systems, and has dramatically impacted our view of land plant evolution. However, a reliance on two-dimensional stelar configurations, and an inconsistency in the inclusion (or exclusion) of secondary tissues somewhat diminished the phylogenetic utility of such work.

More recently, a revival of studies that stress three dimensional architecture of primary tissue systems has set the stage for dramatically increasing the depth with which we understand the vascular tissues of land plants. These studies also allow us to more accurately recognize broad patterns of systematically correlated vascular architectures that may be used to further refine hypotheses of land plant phylogeny. From plant paleontology, we are becoming increasingly aware that conducting tissues have evolved independently in two or more groups of primitive land plants. Nevertheless, the tiny centrarch haplosteles of rhyniophytes provide an archetype for considering broad patterns of stelar changes through time. Such changes have occurred in fundamentally different ways in divergent phylogenetic lineages.

Lycophytes are the most ancient group of land plants with living representatives, and they may be regarded as having vascular architectures that evolved independently of other tracheophytes. Lycophytes display a wide array of exarch protosteles in the stems, and a complex vascular system that characterizes the shoot-derived rooting system of *Isoetes* and of the extinct rhizomorphic lycophytes. Immediately distal to the rhizomorph in *Paurodendron*, protoxylem of the centrarch haplostele divides. Three resulting protoxylem strands extend to the periphery of the xylem in conjunction with divergence of the basal leaf traces. This illustrates the ontogenetic transition from a centrarch stele to the exarch stele, and provides a model for the evolutionary origin of exarch lycophyte steles. It also correlates well with known aspects of apical development under the influence of the terminal meristem in *Lycopodium*.

The evolution of vascular architecture in stems of ferns is well represented by transformational series from solid protosteles to highly dissected dictyosteles. Series occur as chronoclines among Paleozoic representatives of both the Psalixochlaenaceae and Osmundaceae, and also as ontogenetic changes along the length of the stem in extant species. Such stems provide the most convincing evidence for the Jeffreyan concept of siphonosteles with true leaf gaps.

Despite continuing assumptions that eusteles represent highly dissected siphonosteles, the exciting and profound realization that seed plants are both structurally and phylogenetically distinct from ferns has been steadily gaining acceptance. Paleobotanical studies by Beck and others provide convincing evidence that evolution of the seed-plant eustele was associated with longitudinal dissection of a ribbed protostele. These studies demonstrate that the eustele is basically a ring of sympodia lacking true leaf gaps like those of many ferns. They also imply that progymnosperms, rather than ferns, are probably ancestral to seed plants.

Recent phylogenetic analyses have stressed the transition from a protostele to a eustele as an important facet of seed plant evolution. Paleobotanical studies have revealed this to be a gradational change in the degree of longitudinal dissection of metaxylem, for the purpose of character coding the change has been collapsed to a binary transformation in most phylogenetic analyses. In contrast, a survey of the broad range of variation in stelar architecture found among Devonian and Carboniferous lignophytes (progymnosperms + seed plants) suggests that evolution of the eustele was far more complex than previously realized. At the

1

present time five parameters of variation have been recognized among the stem steles of primitive seed ferns, and each may reflect a different aspect of stelar evolution. These parameters are (1) variation in the degree of longitudinal dissection of metaxylem, (2) variation in the ratio of tracheids to parenchyma in primary xylem, (3) variation in protoxylem architecture from a central monopodium to a ring of sympodia, (4) variation in the shape of the stele from distinctly ribbed to polygonal, and (5) variation in stelar diameter. Numbers 1, 2, and 3 probably are of the greatest evolutionary significance.

Although most of these parameters show gradational variations, the change in protoxylem architecture appears to be qualitative in nature. Some protostelic seed ferns display a central protoxylem monopodium from which the leaf trace protoxylem diverges. Other protostelic forms have a ring of protoxylem sympodia, one near the base of each stelar rib, and each of these divides to produce leaf trace protoxylem. Possible evidence for a transition from one architecture to the other occurs in sympodial species where there is an intermittent central protoxylem, and in stems that lack both a central protoxylem and a ring of cauline protoxylem sympodia.

This range of protoxylem architecture is best explained by the hypothesis that protoxylem differentiation is under the influence of several factors (hormones, sugars, etc.) produced at or translocated to centers in either or both of the terminal meristem and leaf primordia. The hypothesis requires that provascular and protoxylem differentiation occur only above a threshold concentration for these influencing factors. Primitive plants without stem/leaf differentiation of the shoot system would have production centers only in the terminal meristem, and thus would have been centrarch. The evolution of leaves from modified branching systems presumably would have led to the progressive transition of auxin production from the terminal meristem to the leaf primordia. Primitive seed plants with a central protoxylem monopodium and marginally mesarch leaf traces are consistent with what could be expected of an early stage in this transition. Forms with discontinuous cauline protoxylem are concordant with what would be expected in stems where the transition was incomplete. And, stems with a ring of protoxylem sympodia, including extant species, are what would be expected where the production of auxin occurs primarily in the leaf primordia.

Observational and experimental data on apical development in *Psilotum*, *Lycopodium*, ferns and seed plants are concordant with this hypothesis, and suggest that lycophytes, ferns and seed plants have alternative control mechanisms of vascular pattern formation that may reflect the independent origin of stem/leaf shoot systems in each. They also provide a basis for hypothesizing the mechanism that operated in the apices of rhyniophytes and trimerophytes. These data and hypothesis are summarized in the table that follows.

Variations in Vascular Tissue Initiation and Differentiation

Site of auxin production: T = Terminal Meristem, L = Leaf Primordia

	[1]Rhy/Tri	*Psilo.*	*Lyco.*	Fil.	S.P.
Provascular Tissue	T	T	T	T	T
(shape)	Rod	Rod	Rod	Cyl.	Cyl.
Procambium	T	T?	T	T	T
(shape)	Rod	Rod	Rod	Cyl.	Cyl.
Differentiation of Xylem and of Phloem	T	T?	T	L	L
Effect of auxin (−)				Cylinder	No Dif.
(+)				Leaf Gaps	Bundles
Protoxylem	Cent.	Ex./Mes.	Ex.	Mes.	[2]Cent.− Mes.

[1] Hypothesized
[2] Primitive by outgroup comparison

The Katherine Esau International Symposium

Plant Structure: Concepts, Connections & Challenges

March 28-31, 1992

Sponsored by
The Division of Biological Sciences
The University of California, Davis

Contributions in support of the Symposium from:

Calgene, Inc.
Blackwell Scientific Publishers, Ltd.
Sandoz Agro, Inc,
Entotech, Inc.

Symposium Organizing Committee:

E.M. Gifford, University of California, Davis
D.G. Gilchrist, University of California, Davis
P.B. Green, Stanford University
D.R. Kaplan, University of California, Berkeley
J.A. Jernstedt, University of California, Davis
W.J. Lucas, University of California, Davis
V.S. Polito (chair), University of California, Davis